Ph.D. Thesis

Novel Function of Lipin and Serotonin Transporter in Development of *Drosophila melanogaster*

PHAM LE ANH TUAN
Kyoto Institute of Technology
September 2020

ABBREVIATIONS

TAG	Triacylglycerides
PAP	Phosphatidate phosphatase
DAG	Diacylglycerides
PPAR	Peroxisome proliferator-activated receptor
KD	Knockdown
ER	Endoplasmic Reticulum
UAS	Upstream Activation Sequence
GFP	Green Fluorescence Protein
IR	Inverted Repeat
SerT	Serotonin transporter
MF	Morphogenetic furrow
PI3K	Phosphatidylinositol 3-kinase
TOR	Target of rapamycin

GENERAL INTRODUCTION

1. Lipin and lipid metabolism

Lipin proteins family

Lipin was first discovered in 1989 by Langner et al. when they report a mutation which caused fatty liver dystrophy in mice [1]. This mutation related to the down-regulated expression of lipoprotein lipase (LPL) and hepatic lipase (HL) in newborn mice. Fld mice were found to have lipodystrophy, high blood triacylglycerides (TAG) level, insulin resistance, fatty liver, and peripheral nerve dysfunction. Peterfy et al. (2001) discovered this mutant gene and called it lipin1 [2]. In 2005, Peterfy et al. also found two lipin isoforms in mice, named as lipin1α and lipin1ß, which possess complementary functions to each other but have different expression patterns and localization in cells. These two lipin1 isoforms encode for proteins with sizes of 98 and 102 kb, respectively [3]. The before functions in early stages of differentiation of adipocyte, while the latter express mainly in mature adipocytes and regulate lipid-related genes and lipogenesis [4]. Lipin1 are also found to be localized in either the cytoplasm or the nucleus of the cells, which lead to a suggestion of dual roles of this protein. The gene for lipin 2 and lipin 3 were later identified with 49 and 46% similarity in amino acid sequence. These three members of lipin express with different patterns in tissues, per their respective roles [5]. Lipin 1 is mainly found in adipose tissue, skeletal muscle, and testis, while presents but in low level in tissues such as the brain, lungs, heart, kidney, and liver. Lipin 2 can be found primarily in the liver. In fld mice, levels of lipin 2 in the liver are dramatically increased, hinting that lipin 2 may be up-regulated in compensation to the absence of lipin 1 [6]. Lipin 3, however, is kept at a low level in most tissues, but it is reported to express highly in pigs liver. In addition, all lipin proteins harbor two regions of high conserved sequence in N- and C-terminal, duped as N-LIP and C-LIP domains, in most organisms. However, only single lipin ortholog were found in invertebrates and yeasts, while two of them were existed in plants [7].

There are two main functions of lipin. One is its role as a phosphatidate phosphatase (PAP) enzyme, which converts phosphatidic acid (PA) to diacylglycerol (DAG) during the formation of stored lipid. All three lipin proteins demonstrate PAP activity with lipin 1 having the strongest magnitude. When

fatty acid levels in the cells raise, lipin will translocate from the cytosol into the endoplasmic reticulum (ER) membrane. Here, they react with PA and catalyze its conversion to DAG [8].

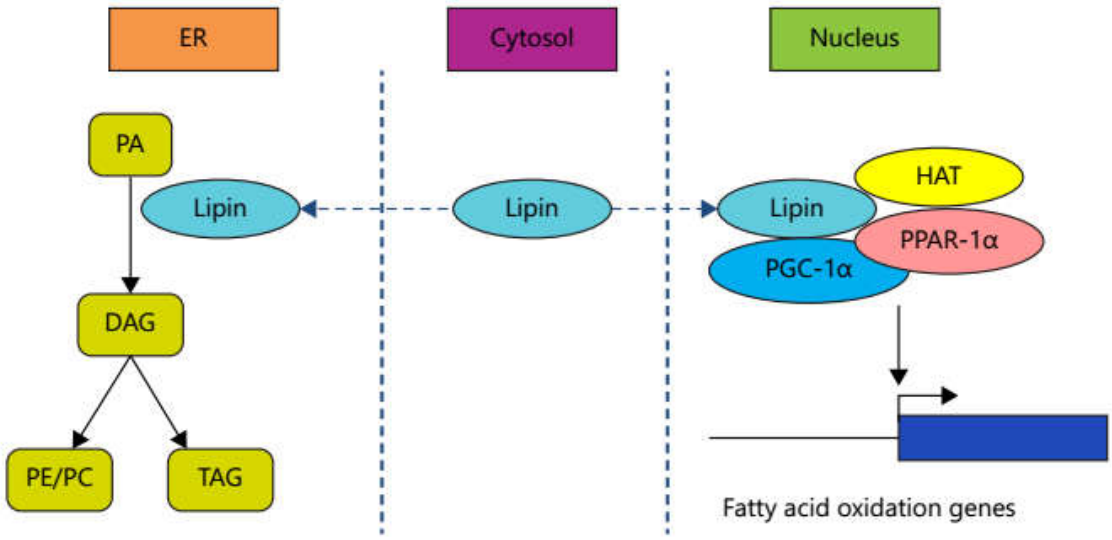

Figure 1. Dual function of lipin [9]

The other function is presented by the capability of lipin to translocate into the nuclear. Studies reported that lipin 1, which induced by phosphorylation can localize in the nucleus of adipocytes and hepatocytes [4,10,11]. Here, lipin acts as a transcriptional co-activator. Lipin 1 interacts with the nuclear receptor peroxisome proliferator-activated receptor α (PPARα) and PPARγ coactivator 1α (PGC-1α) in a complex that modulates fatty acid oxidation gene expression. Besides, recent studies showed that lipin1 can also interact with other nuclear receptors, such as PPARγ, hepatocyte nuclear factor-4α (HNF-4α), glucocorticoid receptor (GR), as well as two non-nuclear receptor transcription factors, including nuclear factor of activated T-cells c4 (NFATc4) and myocyte enhancer factor 2 (MEF2) [11–16]. Kim et al. demonstrated that lipin also works as a transcription suppressor in some contexts. Lipin 1 regulates the recruitment of histone deacetylases to target promoters, which in turn prevents the activity of NFATc4 [15]. Moreover, several studies showed that lipin 3 acts as a transcriptional factor for PPARα, while both lipin 2 and 3 are interact with PPARγ [17,18].

Lipin in Drosophila lipid metabolism

In *Drosophila*, lipid is mainly stored in the insects' unique adipocytes called lipid droplet, in the form of TAG. Lipid plays important roles in physiology and pathophysiology of *Drosophila* such as energy storage, cell-cell signaling, and contribute to the formation of cell membranes.

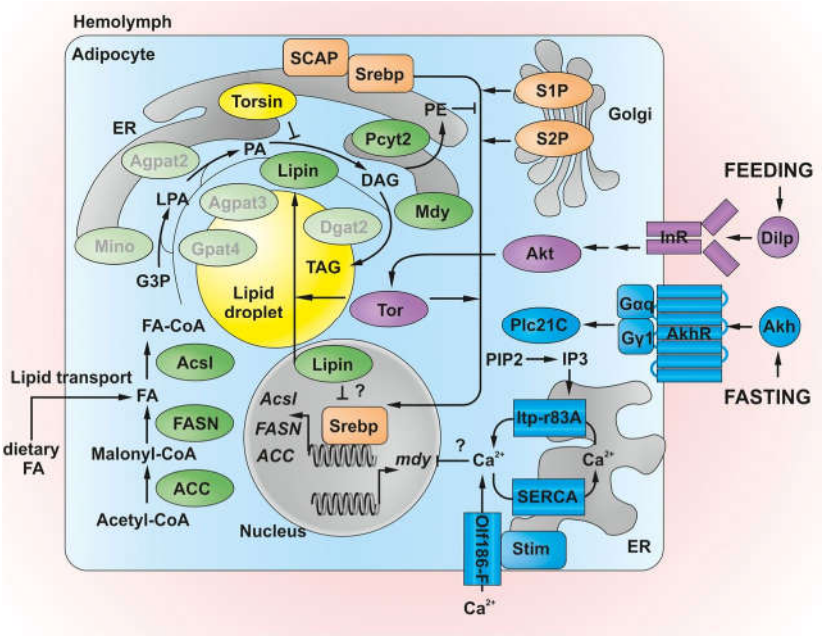

Figure 2. Lipogenesis or the synthesis of stored lipid of Drosophila[19]

In the synthesis of TAG, fatty acids (FAs) are stimulated to FA-CoA by Acsl, and are esterified to lysophosphatidic acid (LPA) and to phosphatidic acid (PA). Lipin de-actives the phosphorylated PA to (DAG), which then esterified by acyltransferases, Mdy, to TAG and stored in lipid droplets. Lipin's ability to move between the cytoplasm and the nucleus is regulated by the target of rapamycin (Tor) kinase, which is under the mediation of insulin pathway regulation via PI3K/Akt under feeding conditions. Lipin also works under the suppression control of Torsin in ER. The transcription factor sterol regulatory element-binding protein (SREBP) increases FA-CoA synthesis by up-regulating the expression *of* Acetyl-CoA-carboxylase (ACC), the FA synthase complex (FASN) and *Acsl*. SREBP activation is either elevated by Tor kinase or inhibited by the membrane lipid PE or also inhibited by nuclear lipin [19].

Regulation of lipin

The lipin proteins activity is mediated by many factors. These factors activate or inhibit lipin via both mRNA transcriptional, protein phosphorylation, and subcellular localization. First, lipin1 phosphorylation by insulin is dependent on the insulin-dependent pathway, PI3K/Akt/TOR signaling pathways [3]. Next, lipin1 expression is increased by synthetic glucocorticoids during adipocyte differentiation. This effect is enhanced by glucagon or cyclic adenosine monophosphate (cAMP) and demoted by insulin [14]. Zhang et al. also found a response of lipin to glucocorticoid [20]. Glucocorticoid bind to the GR, in the lipin1 upstream sequence, allows for lipin activation by synthetic glucocorticoid and dexamethasone. Insulin also a factor that induces the expression of Lipin1 Insulin-sensitizing compounds such as thiazolidinediones and harmine are found to increase lipin levels [21–23]. Sterols also participate in modulating the expression of lipin1 via SREBP and nuclear factor Y (NF-Y). In contrast, lipin1 expression is induced by sterol depletion that controls TAG accumulation through PAP1 activity in the cytosol [24]. In addition, ethanol also increases lipin1 expression in the liver, mainly via SREBP-1 and NF-Y [25].

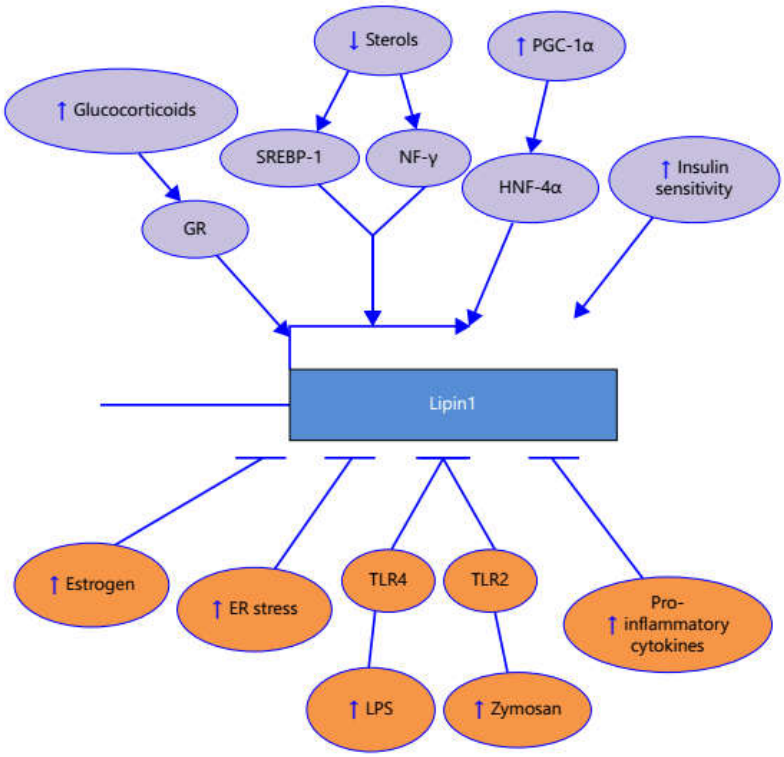

Figure 3. Multiple regulators of lipin [9].

On the other hand, multiple negative regulators were found to suppress lipin1 expression. Studies showed that ER stress inducers (tunicamycin and thapsigargin) inhibit lipin1 expression in 3T3-L1 adipocytes, while activation of PPAR-γ relieves this effect [26]. Interestingly, ER stress induces lipin2 expression in the liver, but hardly affects the adipocytes, indicating the tissue-dependent mechanism [27]. Estrogen significantly reduces the expression of lipin1 in the uterus and liver hinting a potential role of lipin1 in diabetes and reproduction [28]. Additionally, lipopolysaccharide (LPS) and glucan compound, zymosan, decrease lipin1 expression in mouse adipocytes by activating the Toll-like receptors. In 3T3-L1 adipocytes, as responses to pro-inflammatory cytokines such as (TNF-α), interleukin-1ß (IL-1ß), and IFN-γ, Lipin1 expression is downregulated, suggesting lipin potential roles in inflammation [29].

Non-lipid-related function of lipin

Some shreds of evidence suggest the additional function of lipin, besides the lipid metabolism-related ones. As mentioned above, the roles of lipin related to insulin, glucocorticoid, ER stress, diabetes, fertility, and inflammation is suggestive. Additionally, in human, there are several lipin1 mutations were identified: Arg800X, c.297 + 2T>C, and c.1259 + 2T>C, and 2 kb deletion in exons 18 and 19. These mutations cause a lot of phenotypes such as muscle pain, weakness, rhabdomyolysis, and myoglobinuria in children, but interestingly, not lipodystrophy [30,31]. Moreover, a study in HIV patients that exhibit lipodystrophy shows significantly reduced expression of lipin [32]. Taken together, the function of lipin outside lipid metabolism is poorly understood. This statement leads to the investigation of a novel function of lipin in this thesis.

2. The Serotonergic system

Serotonin

The finding of Serotonin was first recorded in 1948 when a factor released from platelets was isolated, purified, and identified as a monoamine by Rapport et al. [33]. It is later becoming clear that serotonin as a neurotransmitter, in addition to the first identified function as a factor in intestinal motility and platelet aggregation. Later, several researchers proposed the relation of Serotonin to

depression [34,35]. This hypothesis suggested that the possibility of affected with depression or mania have a tight connection to the decreasing of serotonergic activity. More specifically, less serotonin release or few serotonin receptors activated or dysfunction in serotonin receptor signal transduction cause the depression. Now, we can define Serotonin (5-hydroxytryptamine – 5-HT) as a monoamine neurotransmitter, derived from tryptophan, mainly found in enterochromaffin cells of the intestine, blood platelet and central nervous system (CNS) [36,37], where it play a major role in the feeling of wellness and happiness. The altered regulation of Serotonin in CNS has been recorded in not only a vast range of behavior functions such as wake/sleep, eating mood, or sexual trends…[38] but also some serious psychotic disorders like depression, bipolar, schizophrenia [39].

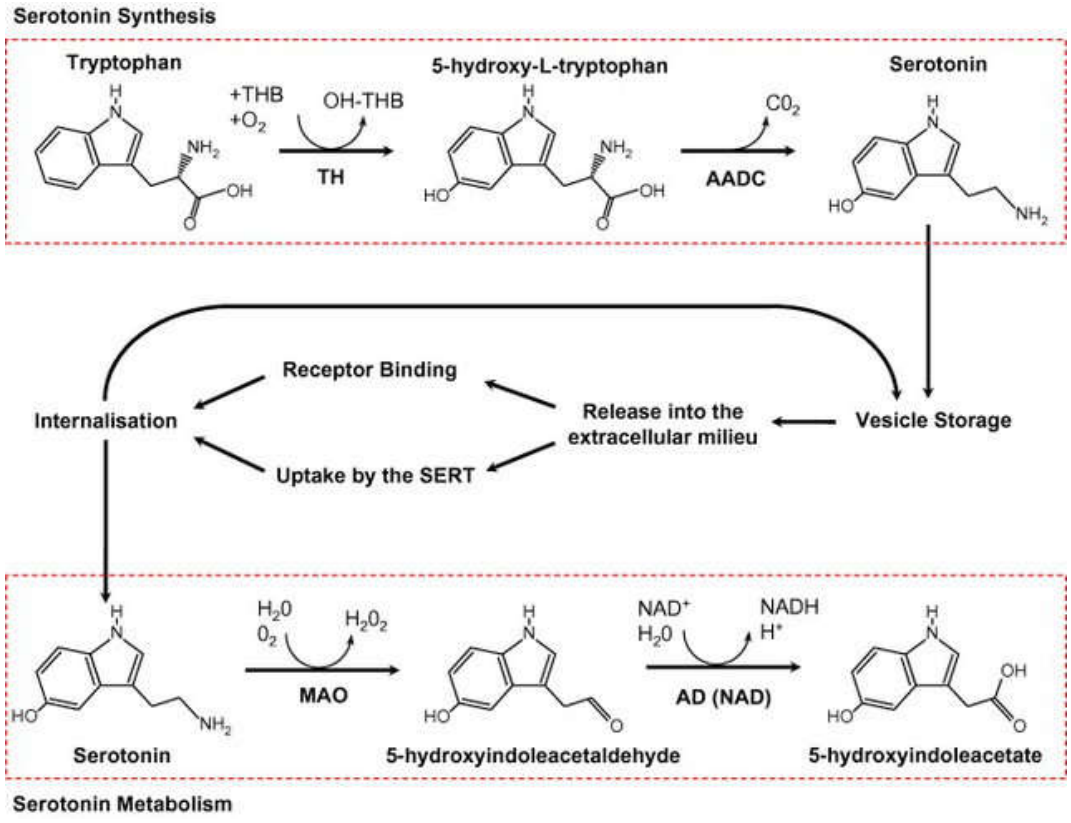

Figure 4. The synthesis and metabolism of Serotonin in human body [40]

Serotonin localizes in both peripheral and neuronal system, which synthesized by different enzymes, Tryptophanhydroxylase-1 (TPH1) and TPH2 respectively [41], and they produce different outcomes. While neuronal Serotonin act as a

neurotransmitter, their peripheral counterpart was considered as a hormonal molecule, which suggests peripheral Serotonin involvement in metabolic processes. The Serotonergic system mainly consists of serotonin, serotonin receptors, and serotonin transporter.

Serotonin receptors

In human, most of the Serotonergic functions is accomplished by the release of Serotonin in specific areas and its activity which mediated at least 14 different receptors [42]. Serotonin receptors are divided base on their distribution, molecular structure, cellular response, and specific function and into seven groups from 5-HTR1 to 5-HTR7 [43]. All Serotonin receptors are G-protein-coupled receptors, except for only 5-HTR3, which is ligand-gated ion channels. Although Serotonin receptors are distributed widely in the CNS and also in a lower level in peripheral organs, the main targets of Serotonergic neurons are the prefrontal cortex and hippocampus, in which express most Serotonin receptors [44,45]. The detailed subtype of Serotonin receptors are listed in Table 1.

Table 1. Classification, distribution and function of Serotonin Receptors

Receptor family	Subtype	Distribution	Mechanism	Cellular response
5-HT1	A,B,D,E,F	CNS, blood vessels	Adenylate cyclase	Inhibitory
5-HT2	A,B,C	CNS, PNS, platelets, blood vessels, smooth muscle	Phospholipase C	Excitatory
5-HT3	A,B	CNS, PNS, GI tract	Ligand-gated ion channel	Excitatory
5-HT4		CNS, PNS	Adenylate cyclase	Excitatory
5-HT5		CNS	Adenylate cyclase	Inhibitory
5-HT6		CNS	Adenylate cyclase	Excitatory
5-HT7		CNS, GI tract, blood vessels	Adenylate cyclase	Excitatory

The work of different Serotonin receptors subtypes via the action of different neuronal networks, even in the same region of the brain, or even in the same synapse can produce opposite results [46].

Serotonin Transporter

Unlike Serotonin receptor, there is only one type of Serotonin transporter (SerT) in the serotonergic system. (SerT) or 5-hydroxytryptamine transporter (5-HTT), by its name, is a monoamine transporter protein in humans responsible for the reuptake of 5-HT from post-synaptic cleft after transmission [47]. SerT protein in humans, which coded by Solute carrier family 6 member 4 (SLC6A4) genes in chromosome 17, consists of 630 amino acids [48]. SerT is a transmembrane transporter; it was divided structurally and functionally into three domains: extracellular domain with several ligand-binding site; transmembrane domain with 12 regions and an intracellular domain with six phosphorylation sites, both the N- and C-termini also are located within. 5-HT transportation depends on extracellular Na+ and extracellular Cl-, these three molecules establish an initial compound, which creates a conformational change in the transporter protein [49]. SerT, from facing outward began moves to an inward position where 5-HT and ions are secreted into neurone cytoplasm [50].

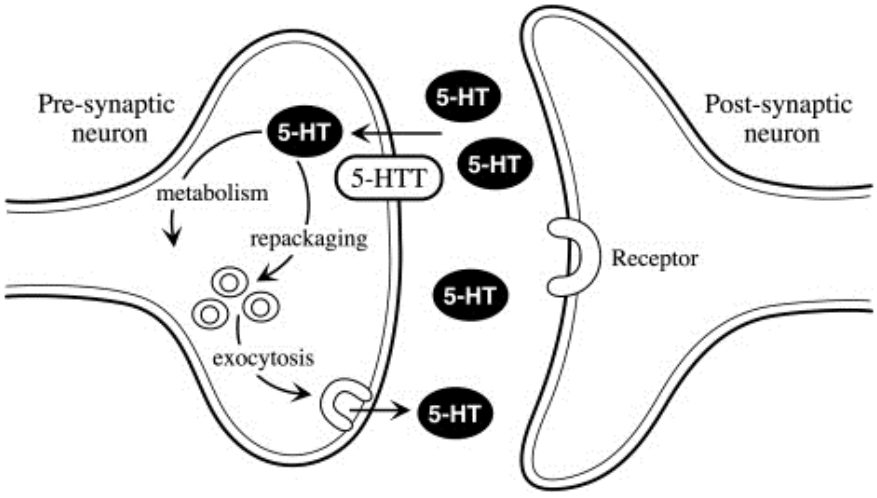

Figure 5. The signaling transmission of Serotonin which involved Serotonin receptors and SerT [51].

SerT functions specifically bind with the regulating of 5-HT, which exists in both CNS and peripheral systems. CNS SerT associates with anxiety and depression-related psychological condition; it is also a target for a large number of antidepressant drugs called selective serotonin reuptake inhibitors (SSRIs) [52]. On the other hand, peripheral SerT has been reported to play a major role in many processes, including heart pumping, appetite regulation, endocrinology and reproduction [53–56]. Still, the research in the peripheral function of SerT remains poorly understood. In chapter 2 of this thesis, we discuss a novel function of SerT in eye development using *Drosophila* model.

3. Drosophila melanogaster as a model to study development

The advantages of Drosophila model

Drosophila is a species of fly, generally known as the common fruit fly or vinegar fly. *Drosophila* was introduced in the laboratory by renowned biologist Thomas H. Morgan in 1908, which then earned him a Nobel Prize for research of chromosome in heredity. Since then, *Drosophila* continues to be widely used for biological research as model organisms for many of its advantages. Firstly, *Drosophila* has small size, thus, easy to culture in standard condition laboratory and low cost, but still achieve high productivity. Also, it takes only ten days for *Drosophila* to produce a new generation and their life cycle is about 70-80 days. Secondly, *Drosophila* possesses only four pairs of chromosomes, but up to 75% of their genome sequence is related to humans, including many genes responsible for psychological, developmental, metabolism… disorders and even cancers. Thirdly, since *Drosophila* is a low-grade organism, researchers can easily manipulate and perform experiments on a large number of individuals without any barrier of moral [57–59]. Last but not least is the emergence of the GAL4-UAS system, a robust biochemical method, developed by Brand A.H. and Perrimon N. in 1993, for studying gene expression, widely used in *Drosophila* [60]. The system contains two parts. One is the Gal4 gene encodes an 881 amino acid protein, recognized as a galactose-induced regulator, in *Saccharomyces cerevisiae* [61,62]. One downside

of GAL4 is having almost to none effect on cells, thus, it requires another necessary part of this system called upstream activation sequence (UAS), a cis-acting regulatory sequence but possess a similar function to an enhancer than a promoter, to where Gal4 will specifically bind and activate gene transcription. Basically, GAL4-UAS system allows us to decide which cell or tissue we want to express on with GAL4-driver and what we want to express with UAS region. For example, to express green fluorescence gene (GFP) within fruit fly wing dorsal area, I would take female flies whose genome contain wing dorsal-specific GAL4 driver (MS1096-GAL4) and cross with male flies whose genome have UAS region next to a target gene. The f1 generation of that two fly strains, which get GAL4 and UAS traits from both parents will have GFP gene express on its wings.

Drosophila model and developmental study

Drosophila is one of the most popular models to study development. Ed Lewis, Christiane Nusslein-Volhard, and Eric Wieschaus, who were awarded Nobel Prize in 1995 for their work on Drosophila development based on the isolation and characterization of mutants of multiple developmental genes. Thanks to their research and many more in the past 25 years, we now have knowledge in a massive database of development-related genes in Drosophila and among those genes, 70% have homologous with humans. Still, there are a lot of genes involved in development remains unknown. The development of *Drosophila* from the embryo to the adult fly is called complete metamorphosis. *Drosophila* life cycle passes through distinct egg, larvae, pupal, and adult stages, and the larva does not resemble the adult. In the larvae stage, the wing and the eye tissue also do not resemble which of the adult, but they exist in the form of imaginal discs. Through the larvae-pupa-adult transition, the discs will transform in shape and size according to the patterns that are strictly regulated by numerous genes. Dysfunction of either one or several of these genes will result in defects in the respective tissue. In the wing, the cells migrate in distinct pattern regarding of their position and region in the disc. The force and the direction of cells migration also responsible for normal wing development. Abnormal growth or dividing of

cells in any region in the eye disc can produce defected phenotypes such as curly wing, notched wing, or complete loss of wing… In the eye tissue, the core of photoreceptor neurons is arrayed in a structure that is accurately repetitive in healthy individuals, small abnormalities in the compound eyes can be easily observed, which makes compound eye tissues ideal for examining cell fate via signaling transduction pathways. To sum up, *Drosophila* is a formidable model to study development. In this thesis, I present two genes, Lipin and SerT, with their novel function in development in two different tissue, the wing, and the eye, respectively.

4. The purpose of this thesis

Development is the key biological processes of life. Throughout an organism's life cycle, numerous genes participate in regulating accurate and stable development. Until now, researchers can only investigate a fraction of these genes. In this thesis, I described the function of two genes, *Lipin* and *SerT*, which have not been found directly related to development. The detail is discussed in two chapters of this thesis as follows.

Chapter 1: *Lipin* is a crucial gene, responsible for lipogenesis or the synthesis of stored lipid. However, in this chapter, I analyzed the vital function of Lipin in the formation of *Drosophila* wing.

Chapter 2: SerT is a well-known gene that takes part in many psychological processes. Although SerT expression in the peripheral system is confirmed, its exact roles remain undiscovered. In this chapter, I unveiled SerT important function in the progress of the developing eye.

5. References

1. Langner, C.A.; Birkenmeier, E.H.; Ben-Zeev, O.; Schotz, M.C.; Sweet, H.O.; Davisson, M.T.; Gordon, J.I. The fatty liver dystrophy (fld) mutation. A new mutant mouse with a developmental abnormality in triglyceride metabolism and associated tissue-specific defects in lipoprotein lipase and hepatic lipase activities. *J. Biol. Chem.* **1989**, *264*, 7994–8003.

2. Peterfy, M.; Phan, J.; Xu, P.; Reue, K. Lipodystrophy in the fld mouse

results from mutation of a new gene encoding a nuclear protein, lipin. *Nat. Genet.* **2001**, *27*, 121–124.
3. Huffman, T.A.; Mothe-Satney, I.; Lawrence, J.C. Insulin-stimulated phosphorylation of lipin mediated by the mammalian target of rapamycin. *Proc. Natl. Acad. Sci. U. S. A.* **2002**, *99*, 1047–1052.
4. Péterfy, M.; Phan, J.; Reue, K. Alternatively spliced lipin isoforms exhibit distinct expression pattern, subcellular localization, and role in adipogenesis. *J. Biol. Chem.* **2005**, *280*, 32883–32889.
5. Carman, G.M.; Han, G.S. Roles of phosphatidate phosphatase enzymes in lipid metabolism. *Trends Biochem. Sci.* 2006, *31*, 694–699.
6. Gropler, M.C.; Harris, T.E.; Hall, A.M.; Wolins, N.E.; Gross, R.W.; Han, X.; Chen, Z.; Finck, B.N. Lipin 2 is a liver-enriched phosphatidate phosphohydrolase enzyme that is dynamically regulated by fasting andobesity in mice. *J. Biol. Chem.* **2009**, *284*, 6763–6772.
7. Reue, K.; Dwyer, J.R. Lipin proteins and metabolic homeostasis. *J. Lipid Res.* 2009, *50*, S109.
8. Reue, K.; Brindley, D.N. Multiple roles for lipins/phosphatidate phosphatase enzymes in lipid metabolism. *J. Lipid Res.* 2008, *49*, 2493–2503.
9. Chen, Y.; Rui, B.-B.; Tang, L.-Y.; Hu, C.-M. Lipin Family Proteins - Key Regulators in Lipid Metabolism. *Ann. Nutr. Metab.* **2015**, *66*, 10–18.
10. Harris, T.E.; Huffman, T.A.; Chi, A.; Shabanowitz, J.; Hunt, D.F.; Kumar, A.; Lawrence, J.C. Insulin controls subcellular localization and multisite phosphorylation of the phosphatidic acid phosphatase, lipin 1. *J. Biol. Chem.* **2007**, *282*, 277–286.
11. Khalil, M.B.; Sundaram, M.; Zhang, H.Y.; Links, P.H.; Raven, J.F.; Manmontri, B.; Sariahmetoglu, M.; Tran, K.; Reue, K.; Brindley, D.N.; et al. The level and compartmentalization of phosphatidate phosphatase-1 (lipin-1) control the assembly and secretion of hepatic VLDL. *J. Lipid Res.* **2009**, *50*, 47–58.
12. Koh, Y.K.; Lee, M.Y.; Kim, J.W.; Kim, M.; Moon, J.S.; Lee, Y.J.; Ahn, Y.H.; Kim, K.S. Lipin1 is a key factor for the maturation and maintenance of adipocytes in the regulatory network with CCAAT/enhancer-binding protein α and peroxisome proliferator-activated receptor γ2. *J. Biol. Chem.* **2008**, *283*, 34896–34906.
13. Chen, Z.; Gropler, M.C.; Mitra, M.S.; Finck, B.N. Complex Interplay between the Lipin 1 and the Hepatocyte Nuclear Factor 4 α (HNF4α) Pathways to Regulate Liver Lipid Metabolism. *PLoS One* **2012**, *7*.
14. Manmontri, B.; Sariahmetoglu, M.; Donkor, J.; Khalil, M.B.; Sundaram, M.; Yao, Z.; Reue, K.; Lehner, R.; Brindley, D.N. Glucocorticoids and cyclic AMP selectively increase hepatic lipin-1 expression, and insulin acts antagonistically. In Proceedings of the Journal of Lipid Research; J Lipid Res, 2008; Vol. 49, pp. 1056–1067.
15. Kim, H.B.; Kumar, A.; Wang, L.; Liu, G.-H.; Keller, S.R.; Lawrence, J.C.; Finck, B.N.; Harris, T.E. Lipin 1 Represses NFATc4 Transcriptional Activity in Adipocytes To Inhibit Secretion of Inflammatory Factors. *Mol. Cell. Biol.* **2010**, *30*,

3126–3139.
16. Liu, G.H.; Gerace, L. Sumoylation regulates nuclear localization of lipin-1α in neuronal cells. *PLoS One* **2009**, *4*.
17. Finck, B.N.; Gropler, M.C.; Chen, Z.; Leone, T.C.; Croce, M.A.; Harris, T.E.; Lawrence, J.C.; Kelly, D.P. Lipin 1 is an inducible amplifier of the hepatic PGC-1α/PPARα regulatory pathway. *Cell Metab.* **2006**, *4*, 199–210.
18. Donkor, J.; Zhang, P.; Wong, S.; O'Loughlin, L.; Dewald, J.; Kok, B.P.C.; Brindley, D.N.; Reue, K. A conserved serine residue is required for the phosphatidate phosphatase activity but not the transcriptional coactivator functions of lipin-1 and lipin-2. *J. Biol. Chem.* **2009**, *284*, 29968–29978.
19. Heier, C.; Kühnlein, R.P. Triacylglycerol metabolism in drosophila melanogaster. *Genetics* **2018**, *210*, 1163–1184.
20. Zhang, P.; O'Loughlin, L.; Brindley, D.N.; Reue, K. Regulation of lipin-1 gene expression by glucocorticoids during adipogenesis. *J. Lipid Res.* **2008**, *49*, 1519–1528.
21. Waki, H.; Park, K.W.; Mitro, N.; Pei, L.; Damoiseaux, R.; Wilpitz, D.C.; Reue, K.; Saez, E.; Tontonoz, P. The Small Molecule Harmine Is an Antidiabetic Cell-Type-Specific Regulator of PPARγ Expression. *Cell Metab.* **2007**, *5*, 357–370.
22. Yao-Borengasser, A.; Rasouli, N.; Varma, V.; Miles, L.M.; Phanavanh, B.; Starks, T.N.; Phan, J.; Spencer, H.J.; McGehee, R.E.; Reue, K.; et al. Lipin expression is attenuated in adipose tissue of insulin-resistant human subjects and increases with peroxisome proliferator-activated receptor γ activation. *Diabetes* **2006**, *55*, 2811–2818.
23. Festuccia, W.T.; Blanchard, P.G.; Turcotte, V.; Laplante, M.; Sariahmetoglu, M.; Brindley, D.N.; Deshaies, Y. Depot-specific effects of the PPARγ agonist rosiglitazone on adipose tissue glucose uptake and metabolism. *J. Lipid Res.* **2009**, *50*, 1185–1194.
24. Ishimoto, K.; Nakamura, H.; Tachibana, K.; Yamasaki, D.; Ota, A.; Hirano, K.I.; Tanaka, T.; Hamakubo, T.; Sakai, J.; Kodama, T.; et al. Sterol-mediated regulation of human lipin 1 gene expression in hepatoblastoma cells. *J. Biol. Chem.* **2009**, *284*, 22195–22205.
25. Hu, M.; Wang, F.; Li, X.; Rogers, C.Q.; Liang, X.; Finck, B.N.; Mitra, M.S.; Zhang, R.; Mitchell, D.A.; You, M. Regulation of hepatic lipin-1 by ethanol: Role of AMP-activated protein kinase/sterol regulatory element-binding protein 1 signaling in mice. *Hepatology* **2012**, *55*, 437–446.
26. Takahashi, N.; Yoshizaki, T.; Hiranaka, N.; Suzuki, T.; Yui, T.; Akanuma, M.; Kanazawa, K.; Yoshida, M.; Naito, S.; Fujiya, M.; et al. Endoplasmic reticulum stress suppresses lipin-1 expression in 3T3-L1 adipocytes. *Biochem. Biophys. Res. Commun.* **2013**, *431*, 25–30.
27. Ryu, D.; Seo, W.Y.; Yoon, Y.S.; Kim, Y.N.; Kim, S.S.; Kim, H.J.; Park, T.S.; Choi, C.S.; Koo, S.H. Endoplasmic reticulum stress promotes LIPIN2-dependent hepatic insulin resistance. *Diabetes* **2011**, *60*, 1072–1081.
28. Gowri, P.M.; Sengupta, S.; Bertera, S.; Katzenellenbogen, B.S. Lipin1 regulation by estrogen in uterus and liver: Implications for diabetes and fertility.

Endocrinology **2007**, *148*, 3685–3693.
29. Lu, B.; Lu, Y.; Moser, A.H.; Shigenaga, J.K.; Grunfeld, C.; Feingold, K.R. LPS and proinflammatory cytokines decrease lipin-1 in mouse adipose tissue and 3T3-L1 adipocytes. *Am. J. Physiol. - Endocrinol. Metab.* **2008**, *295*.
30. Zeharia, A.; Shaag, A.; Houtkooper, R.H.; Hindi, T.; de Lonlay, P.; Erez, G.; Hubert, L.; Saada, A.; de Keyzer, Y.; Eshel, G.; et al. Mutations in LPIN1 Cause Recurrent Acute Myoglobinuria in Childhood. *Am. J. Hum. Genet.* **2008**, *83*, 489–494.
31. Michot, C.; Hubert, L.; Romero, N.B.; Gouda, A.; Mamoune, A.; Mathew, S.; Kirk, E.; Viollet, L.; Rahman, S.; Bekri, S.; et al. Study of LPIN1, LPIN2 and LPIN3 in rhabdomyolysis and exercise-induced myalgia. *J. Inherit. Metab. Dis.* **2012**, *35*, 1119–1128.
32. Lindegaard, B.; Larsen, L.F.; Hansen, A.B.E.; Gerstoft, J.; Pedersen, B.K.; Reue, K. Adipose tissue lipin expression levels distinguish HIV patients with and without lipodystrophy. *Int. J. Obes.* **2007**, *31*, 449–456.
33. Rapport, M.M.; Green, A.A.; Page, I.H. Crystalline serotonin. *Science (80-.).* **1948**, *108*, 329–330.
34. Nelson, J.C.; Charney, D.S. The symptoms of major depressive illness. *Am. J. Psychiatry* **1981**, *138*, 1–13.
35. Meltzer, H. Serotonergic dysfunction in depression. In Proceedings of the British Journal of Psychiatry; Cambridge University Press, 1989; Vol. 155, pp. 25–31.
36. Gershon, M.D.; Tack, J. The Serotonin Signaling System: From Basic Understanding To Drug Development for Functional GI Disorders. *Gastroenterology* **2007**, *132*, 397–414.
37. Iurescia, S.; Seripa, D.; Rinaldi, M. Looking Beyond the 5-HTTLPR Polymorphism: Genetic and Epigenetic Layers of Regulation Affecting the Serotonin Transporter Gene Expression. *Mol. Neurobiol.* 2017, *54*, 8386–8403.
38. Jacobs, B.L.; Azmitia, E.C. Structure and function of the brain serotonin system. *Physiol. Rev.* 1992, *72*, 165–230.
39. Baou, M.; Boumba, V.A.; Petrikis, P.; Rallis, G.; Vougiouklakis, T.; Mavreas, V. A review of genetic alterations in the serotonin pathway and their correlation with psychotic diseases and response to atypical antipsychotics. *Schizophr. Res.* 2016, *170*, 18–29.
40. Ruddell, R.G.; Mann, D.A.; Ramm, G.A. The function of serotonin within the liver. *J. Hepatol.* 2008, *48*, 666–675.
41. Visser, A.K.D.; Ramakrishnan, N.K.; Willemsen, A.T.M.; Di Gialleonardo, V.; De Vries, E.F.J.; Kema, I.P.; Dierckx, R.A.J.O.; Van Waarde, A. 11C5-HTP and microPET are not suitable for pharmacodynamic studies in the rodent brain. *J. Cereb. Blood Flow Metab.* **2014**, *34*, 118–125.
42. Nichols, D.E.; Nichols, C.D. Serotonin receptors. *Chem. Rev.* **2008**, *108*, 1614–1641.
43. McCorvy, J.D.; Roth, B.L. Structure and function of serotonin G protein-coupled receptors. *Pharmacol. Ther.* 2015, *150*, 129–142.

44. Celada, P.; Victoria Puig, M.; Artigas, F. Serotonin modulation of cortical neurons and networks. *Front. Integr. Neurosci.* **2013**, *7*.
45. LC, B.; A, R.; R, M.; G, G.-A. Serotonin Receptors in Hippocampus. *ScientificWorldJournal.* **2012**, *2012*.
46. Leiser, S.C.; Li, Y.; Pehrson, A.L.; Dale, E.; Smagin, G.; Sanchez, C. Serotonergic Regulation of Prefrontal Cortical Circuitries Involved in Cognitive Processing: A Review of Individual 5-HT Receptor Mechanisms and Concerted Effects of 5-HT Receptors Exemplified by the Multimodal Antidepressant Vortioxetine. *ACS Chem. Neurosci.* 2015, *6*, 970–986.
47. Oh, C.M.; Namkung, J.; Go, Y.; Shong, K.E.; Kim, K.; Kim, H.; Park, B.Y.; Lee, H.W.; Jeon, Y.H.; Song, J.; et al. Regulation of systemic energy homeostasis by serotonin in adipose tissues. *Nat. Commun.* **2015**, *6*.
48. Wang, Y.M.; Chang, Y.; Chang, Y.Y.; Cheng, J.; Li, J.; Wang, T.; Zhang, Q.Y.; Liang, D.C.; Sun, B.; Wang, B.M. Serotonin transporter gene promoter region polymorphisms and serotonin transporter expression in the colonic mucosa of irritable bowel syndrome patients. *Neurogastroenterol. Motil.* **2012**, *24*.
49. Rudnick, G.; Clark, J. From synapse to vesicle: The reuptake and storage of biogenic amine neurotransmitters. *BBA - Bioenerg.* 1993, *1144*, 249–263.
50. Rudnick, G. Structure/function relationships in serotonin transporter: new insights from the structure of a bacterial transporter. *Handb Exp Pharmacol* **2006**, 59–73.
51. Haney, E.M.; Calarge, C.; Bliziotes, M.M. Clinical Implications of Serotonin Regulation of Bone Mass. In *Translational Endocrinology of Bone*; Elsevier Inc., 2013; pp. 189–198 ISBN 9780124157842.
52. Brindley, R.L.; Bauer, M.B.; Blakely, R.D.; Currie, K.P. Serotonin and Serotonin Transporters in the Adrenal Medulla: A Potential Hub for Modulation of the Sympathetic Stress Response. *ACS Chem Neurosci* **2017**.
53. Genet, N.; Billaud, M.; Rossignol, R.; Dubois, M.; Gillibert-Duplantier, J.; Isakson, B.E.; Marthan, R.; Savineau, J.P.; Guibert, C. Signaling Pathways Linked to Serotonin-Induced Superoxide Anion Production: A Physiological Role for Mitochondria in Pulmonary Arteries. *Front Physiol* **2017**, *8*, 76.
54. Solmi, M.; Gallicchio, D.; Collantoni, E.; Correll, C.U.; Clementi, M.; Pinato, C.; Forzan, M.; Cassina, M.; Fontana, F.; Giannunzio, V.; et al. Serotonin transporter gene polymorphism in eating disorders: Data from a new biobank and META-analysis of previous studies. *World J Biol Psychiatry* **2016**, *17*, 244–257.
55. Yamakawa, K.; Matsunaga, M.; Isowa, T.; Ohira, H. Serotonin transporter gene polymorphism modulates inflammatory cytokine responses during acute stress. *Sci Rep* **2015**, *5*, 13852.
56. Coleman, J.A.; Green, E.M.; Gouaux, E. X-ray structures and mechanism of the human serotonin transporter. *Nature* **2016**, *532*, 334–339.
57. Diop, S.B.; Bodmer, R. Drosophila as a model to study the genetic mechanisms of obesity-associated heart dysfunction. *J Cell Mol Med* **2012**, *16*, 966–971.
58. Reiter, L.T.; Potocki, L.; Chien, S.; Gribskov, M.; Bier, E. A systematic

analysis of human disease-associated gene sequences in Drosophila melanogaster. *Genome Res.* **2001**, *11*, 1114–1125.
59. Reiter, L.T.; Potocki, L.; Chien, S.; Gribskov, M.; Bier, E. A systematic analysis of human disease-associated gene sequences in Drosophila melanogaster. *Genome Res* **2001**, *11*, 1114–1125.
60. Brand, A.H.; Perrimon, N. Targeted gene expression as a means of altering cell fates and generating dominant phenotypes. *Development* **1993**, *118*, 401–415.
61. Laughon, A.; Gesteland, R.F. Primary structure of the Saccharomyces cerevisiae GAL4 gene. *Mol Cell Biol* **1984**, *4*, 260–267.
62. Laughon, A.; Driscoll, R.; Wills, N.; Gesteland, R.F. Identification of two proteins encoded by the Saccharomyces cerevisiae GAL4 gene. *Mol. Cell. Biol.* **1984**, *4*, 268–275.

Chapter 1. The Function of Lipin in the Wing Development of *Drosophila melanogaster*

1. Introduction

The phospholipid components of biological membranes are pivotal for cellular processes including growth, differentiation, and transport, as phospholipids participate in important signaling cascades [1–3]. Phospholipid synthesis involves phosphatidic acid (PA) and diacylglycerol (DAG), both of which have critical roles in signaling cascades, energy storage, and lipid anabolism pathways [4]. Carman et al. (2017) showed that PA is degraded by conversion into DAG, the direct precursor for producing phosphatidylcholine and phosphatidylethanolamine [5]. Moreover, PA can be converted to cytidine diphosphate diacylglycerol (CDP-DAG), the precursor for the production of PA, phosphatidylglycerol, cardiolipin, and phosphatidylinositol [6]. They inhibit the reactions of DNA polymerases, which are essential for DNA replication [7].

In the cytoplasm, lipins function as a type of phosphatidate phosphatases (PAP1 enzymes) that catalyze Mg^{2+}-dependent dephosphorylation of PA to form DAG at the endoplasmic reticulum (ER) membrane. Thus, lipins have an essential role in coordinating the balance between PA and DAG [8] and are involved in the formation of triacylglycerol (TAG) [9], which plays a central role in cellular lipid storage [10]. In the nucleus, lipin works as a transcriptional co-activator in a complex with peroxisome proliferator-activated receptor γ coactivator-1α (PGC-1α) and peroxisome proliferator-activated receptor α (PPARα) [11,12], which are master regulators of genes related to mitochondrial biogenesis and fatty acid oxidation [11,12]. The function of lipins is evolutionarily conserved from eukaryotes to mammals [13]. In humans, the lipin protein family consists of three members: lipin 1, 2, and 3 [14,15], which are localized within different tissues. Lipin 1, the best characterized among the three, resides in the fat tissues and cardiac and skeletal muscles, whereas lipin 2 and lipin 3 are detected in the liver [16–18] and intestine [17], respectively. A previous study demonstrated that lipins 1 and 2 in mammalian cells are inhibited by phosphorylation during mitosis, causing a reduction in the cellular PAP1 activity during cell division [13]. This

study suggested the possibility that a decrease in PAP1 activity could contribute to the inhibition of phospholipid accumulation prior to cell division. In yeast, lipin can negatively control the synthesis of phosphatidylcholine and other phospholipids by suppressing key phospholipid biosynthesis pathway genes [11]. The subsequent abnormalities of phospholipid synthesis may indirectly affect DNA replication [19]. Moreover, loss of lipin induces the overgrowth of intracellular membranes, affects the envelopes of nuclei and peripheral ER, and leads to defective chromosome segregation [11,20]. Genetic knockdown of *lipin 1* in mice induces lipodystrophy and insulin resistance and alters hepatic metabolism [21], whereas transgenic mice overexpressing lipin 1 show an obese phenotype [22]. In *Drosophila,* decreased expression of *Drosophila* lipin (dLipin) was found to affect the normal development of the fat body, which is the major tissue for TAG storage in invertebrates [23], and resulted in down-regulation of the insulin-receptor-controlled PI3K-Akt pathway and increased hemolymph sugar levels [24]. Schmitt et al. indicated that insulin and target of rapamycin complex 1 (TORC-1) pathways independently regulate nuclear translocation of dLipin [24]. In mammals, blocking TORC1 dephosphorylates lipin 1, leading to its translocation from the cytoplasm into the nucleus, where it affects nuclear protein levels, but not mRNA levels, of the transcription factor sterol regulatory element-binding protein 1 (SREBP1), which is a main regulator of genes that are related to the biosynthesis of fatty acid, cholesterol, TAG, and phospholipid [25].

The cell cycle consists of a series of events that lead to cell division and the duplication of cellular DNA, which is then precisely separated into daughter cells. There are two main regulators of cell cycle progression, cyclins and cyclin-dependent kinases (CDKs) [26]. Cyclins are divided into four classes. G1/S cyclins, S cyclins, and M cyclins are directly related to the control of cell cycle events, whereas G1 cyclins control the entry into the cell cycle in response to extracellular growth factors and mitosis [27]. CDKs contain a serine/threonine-specific catalytic core and associates with cyclins to regulate kinase activity and substrate specificity [28], promoting S phase progression,

checkpoint, and mitosis [26,27,29,30]. For example, CDK2 is important for S phase progression whereas CDK1 is essential for the G2 checkpoint and mitosis [31–33]. The cell cycle contains several specific checkpoints to monitor and control its progression and to allow verification of phase processes and repair of DNA damage [34–36]. There are three specific checkpoints for damaged or incompletely replicated DNA: G1/S, G2/M, and intra-S checkpoints [27]. The current study aimed to reveal the role of lipins in development using *Drosophila melanogaster*. Specifically, we investigated the role of dLipin in cell cycle progression during wing formation in *D. melanogaster*.

2. Results

2.1. Localization of dLipin in Wing Imaginal Disc

It has been reported that dLipin resides on the wing imaginal disc of *D. melanogaster* [23]. To determine a specific dLipin location on the wing imaginal disc, we stained the wing imaginal discs from 3rd-instar larvae of the wild-type yellow-white *(yw)* strain with an anti-dLipin antibody. We found that dLipin signals are detected throughout the wing imaginal discs with relatively stronger signals in the anterior part of the margin and notum, and slightly lesser signals in the wing pouch and hinge (Figure 1a). In subsequent studies, we analyzed dLipin in the margin of the wing disc, which later becomes the wing margin of the adult wing blade. Lehmann's group has reported that dLipin is translocated from the cytoplasm to nucleus in fat tissue under starvation conditions [23,24]. We also confirmed that dLipin is detected in both the cytoplasm and the nuclei of fat body cells in starved conditions by immunostaining (Figure S1). In contrast, immunostaining of wing imaginal discs from 3rd-instar larvae, in starved or fed condition, showed that unlike in fat tissue, dLipin did not appear to translocate into the nucleus of wing imaginal disc cells (Figure 1d–i).

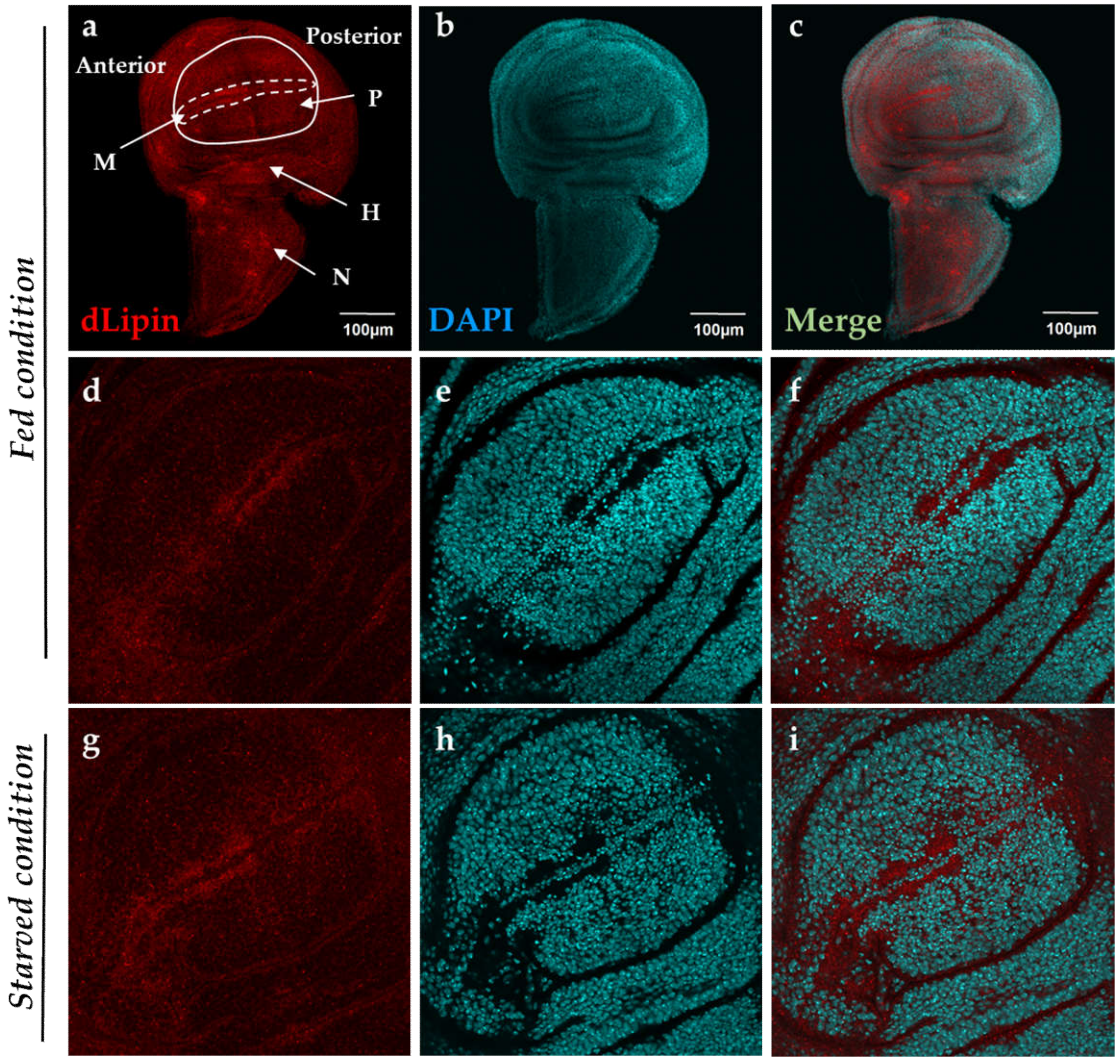

Figure 1. Localization of *Drosophila* lipin (dLipin) protein on the wing imaginal disc of the *yw* strain. Wing imaginal discs of 3rd-instar larvae were stained with 4',6-diamidino-2-phenylindole (DAPI) (**b, e, h**) to visualize DNA, and rabbit anti-dLipin antibody (**a, d, g**) followed by anti-rabbit IgG Alexa Fluor™ 594 antibody. Merged images of DAPI and antibody staining (**c, f, i**). Fed condition (**a**–**f**), starved condition (**g**–**i**). The images are representative among images of 10–20 wing imaginal discs. dLipin protein was expressed in whole wing imaginal disc, with particularly high expression in the anterior part of the margin (M), and notum (N), albeit slightly lower expression in the wing pouch (P) and hinge (H) (**a**–**c**). The dotted circle indicates the margin of the wing imaginal disc. The wing pouch demarcated with the white line is shown in **d**, **g**. dLipin was not detected in the nuclei of wing imaginal discs of 3rd-instar larvae either in the fed or starved

state (**d**–**i**). Scale bar, 50 μm.

2.2. Knockdown of dLipin Disrupts Normal Wing Pattern Formation

A previous study showed that lack of dLipin resulted in a lethal phenotype at late larval and pupal stages of *Drosophila* [23]. To determine whether dLipin is required for the development of specific tissues, two RNAi fly lines, UAS-*dLipin*-IR$_{277\text{-}380}$ and *dLipin*-IR$_{265\text{-}272}$, were crossed with various GAL4 driver lines that express GAL4 in selective tissues. Target sequences for these two RNAi sequences were designed to have no off-target effects (Vienna Drosophila Resource Center and online dsCheck software http://dscheck.rnai.jp). First, we overexpressed GFP using *Sd*-GAL4 drivers to confirm the region in the wing imaginal disc where GAL4 is expressed. Similar to previous reports [37–39], stronger GFP signals were detected in the margin area and wing pouch of 3rd-instar larvae driven by *Sd*-GAL4, suggesting effective knockdown of *dLipin* in this region of the knockdown fly (Figure S2). Furthermore, we checked the expression levels of dLipin mRNA and protein in the wing disc of 3rd-instar larvae by qRT-PCR and immunostaining, respectively. As shown in Figure S3, dLipin mRNA and protein levels were significantly reduced in the wing discs of knockdown fly lines, suggesting efficient knockdown of *dLipin* in wing imaginal discs of both knockdown flies.

Having confirmed the efficient knockdown of dLipin in the margin area and wing pouch of 3rd-instar larvae driven by *Sd*-GAL4, we next observed the phenotype of wings of *dLipin*-knockdown flies. The phenotypic observation demonstrated that the two different lines with *dLipin*-knockdown (*dLipin*-kd; *Sd* > *dLipin*-IR$_{265\text{-}272}$ and *Sd* > *dLipin*-IR$_{277\text{-}380}$) in the wing disc mediated by *sd*-GAL4 led to atrophied wing formation, notched and down-curled wings, along with reduction in size (Figure 2b,b',c,c'). Statistical analysis showed that the reduction of wing size by *dLipin*-kd was significant as compared to that of the control fly (Figure 2e). In contrast, the flies with *dLipin*-knockdown in the nervous system using the *elave*-GAL4 driver, or in hemocytes using *Hml*Δ-GAL4 or *He*-GAL4, showed no detectable phenotype , suggesting that *dLipin* has no or minimal role in the

development of these tissues. However, the possibility of low-level expression of GAL4 protein leading to the insufficient *dLipin*-kd in these tissues could not be excluded. Thus, we confirmed that the *dLipin*-kd phenotypes were caused by the deficient expression of dLipin selectively in the margin area and wing pouch of the wing disc.

To confirm whether *dLipin*-kd phenotypes, notching, and curly wing blades were related to the deficient TAG level, we measured the TAG contents of whole-wing imaginal discs of control and knockdown flies. It was found that the TAG level was significantly reduced in *dLipin*-kd (Figure 2f), compared to that of the control. These data suggested that the atrophied wing blade formation might be related to the deficient TAG level in the wing imaginal disc. Then, to confirm this point, the *dLipin*-kd (*Sd* > *dLipin*-$IR_{265\text{-}272}$) eggs were hatched on high-fat diet food, the hatched larvae were cultured on the same food, and then, the TAG levels of the whole-wing imaginal disc of 3rd-instar larvae and adult wing blades were analyzed. Notably, the *dLipin*-kd phenotypes were not rescued by high-fat diet food (Figure 2d,d',e), even though TAG contents of wing discs of *Sd* > *dLipin*-$IR_{265\text{-}272}$ flies were increased by high-fat diet. This demonstrated that the abnormal wing formation in *dLipin*-knockdown flies might not be caused by deficient TAG in the wing imaginal disc.

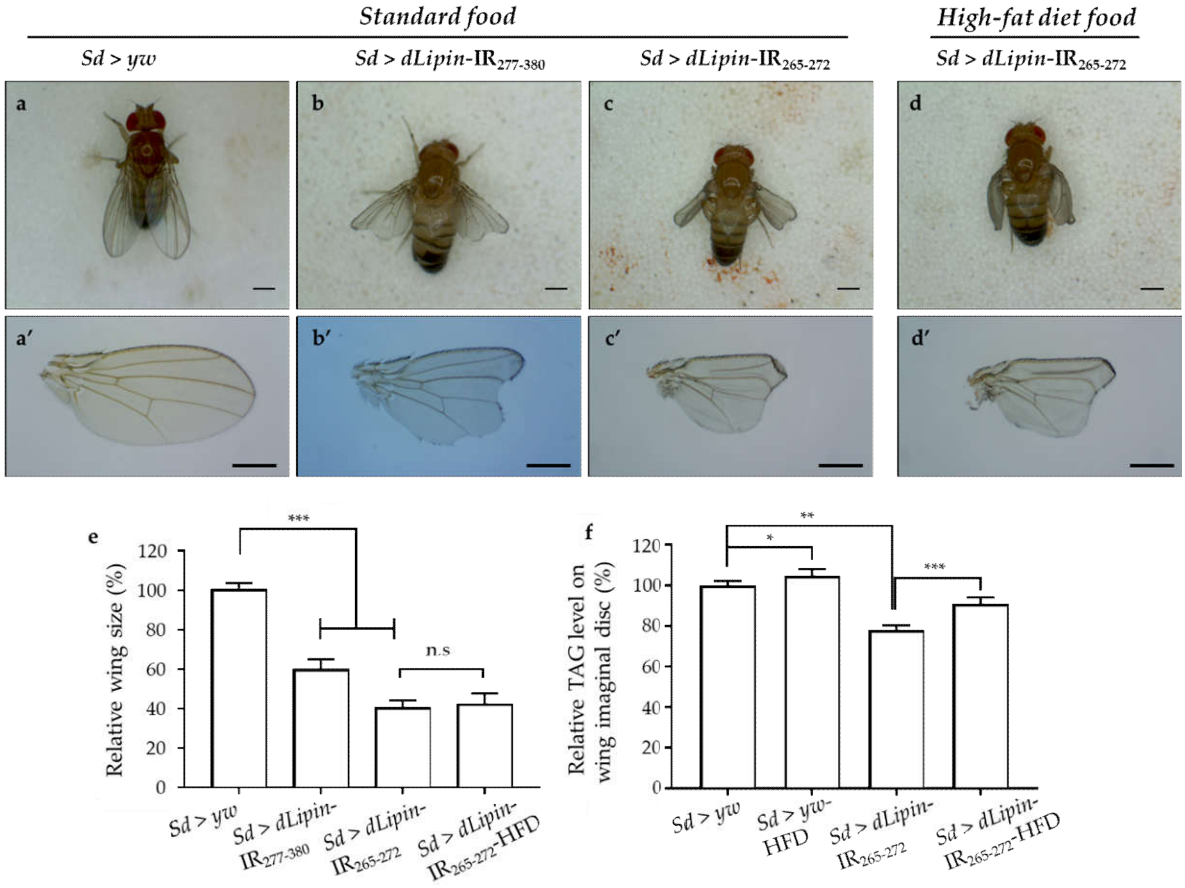

Figure 2. *dLipin*-kd selectively causes atrophied wing development in the wing imaginal disc. Micrographs of adult flies (**a**–**d**) and wing blades (**a'**–**d'**) are shown. The control flies were obtained by crossing the *Sd*-GAL4 drivers with the *yw* strain (**a, a'**). Wings of *dLipin*-kd flies (*Sd* > *dLipin*-IR$_{265\text{-}272}$ and *Sd* > *dLipin*-IR$_{277\text{-}380}$) showed wing notching and curl (**b, b'**, **c, c'**). *dLipin*-kd phenotypes were not recused by the administration of a high-fat diet (**d, d'**). The size of the wing blade was analyzed using ImageJ software. The relative size of the *dLipin*-kd fly wing to that of control fly are shown (n = 50 for each genotype) (**e**). The relative triacylglycerol (TAG) level of the *dLipin*-kd wing imaginal disc to that of the control was analyzed using 100 imaginal discs (n = 4 for each genotype) (**f**). Data are expressed as the means ± S.D. The statistical significance of the difference between control and *dLipin*-kd flies was evaluated using t-test and one-way ANOVA. Scale bar, 0.5 mm; *, p = 0.03, **, p < 0.02, ***, p < 0.01; n.s, no significant; IR, inverted repeat, HFD, high-fat diet. Genotypes: *Sd*-GAL4/y; +;

+ (**a, a'**), *Sd*-GAL4/y; UAS-*dLipin*-IR$_{277-380}$/+; + (**b, b'**), *Sd*-GAL4/y; UAS-*dLipin*-IR$_{265-272}$/+; + (**c, c', d, d'**).

2.3. Knockdown of dLipin Inhibits Cells from Entering M Phase

To reveal the mechanism underlying the aberrant wing formation in *dLipin*-kd flies, we analyzed the effect of *dLipin* knockdown on the cell cycle progression in wing imaginal discs. We first determined the number of cells in S phase by 5-Ethynyl-2′-deoxyuridine (EdU) pulse labeling [40], and found a significant increase in the EdU-positive cell in the wing margin of *dLipin*-kd wing imaginal discs (Figure 3d,g,j) as compared to that in the control flies (Figure 3a,j).

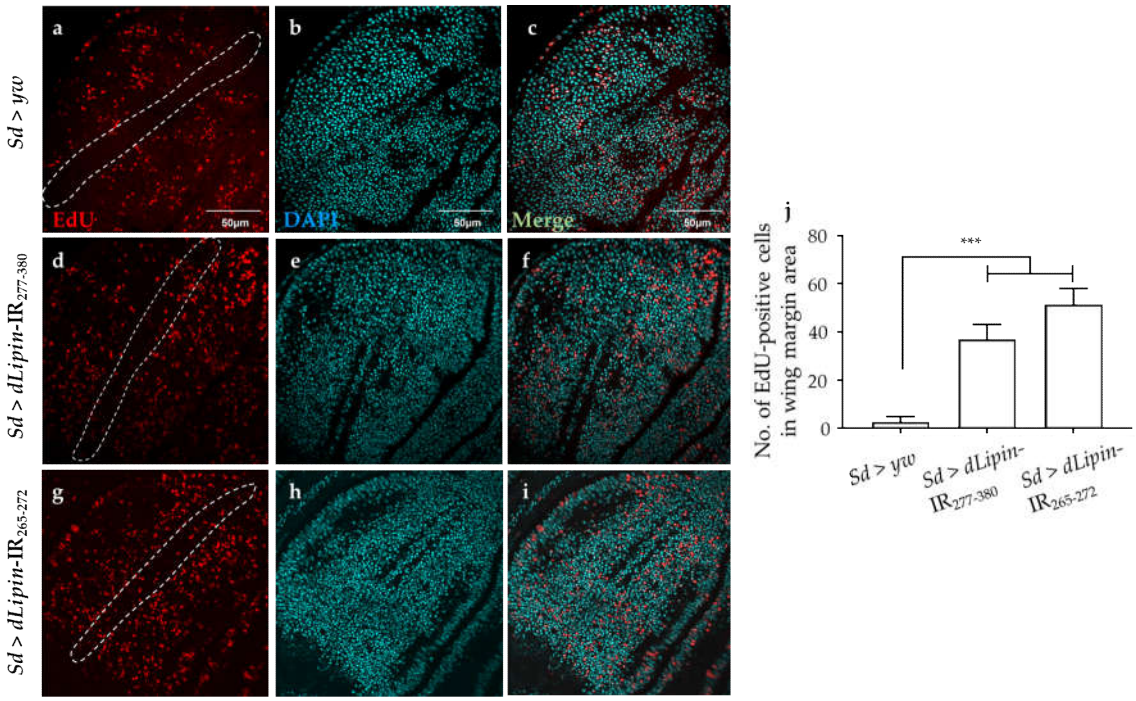

Figure 3. Knockdown of *dLipin* induces accumulation of cells in S phase. Wing imaginal discs from 3rd-instar larvae of control (*Sd* > *yw*) and *dLipin*-kd flies (*Sd* > *dLipin*-IR$_{265-272}$ and *Sd* > *dLipin*-IR$_{277-380}$) were stained with DAPI to visualize the DNA (**b, e, h**) and click-iT 5-Ethynyl-2′-deoxyuridine (EdU) Alexa Fluor™ 594 (**a, d, g**). Merged images of DAPI and EdU staining are shown (**c, f, i**). The number of EdU-positive cells in S phase in the wing margin area of 3rd-instar larvae, circled with a dotted line, were analyzed using MetaMorph software (n = 10 for each genotype) (**j**). Dotted line indicates the margin of the wing imaginal disc. Data are expressed as the means ± S.D. The statistical significance of the

difference between control and *dLipin*-kd flies was evaluated using one-way ANOVA. Scale bar, 50 μm. ***, $p < 0.01$. IR, inverted repeat. Genotypes: *Sd*-GAL4/+; +; + (**a**–**c**), *Sd*-GAL4/+; UAS-*dLipin*-IR$_{277\text{-}380}$/+; + (**d**–**f**), *Sd*-GAL4/+; UAS-*dLipin*-IR$_{265\text{-}272}$/+; + (**g**–**i**).

We next analyzed the number of mitotic cells by immunostaining the wing imaginal discs with an anti-PH3S10 antibody, which is a hallmark of initiation of mitosis [41,42]. Compared to the control (Figure 4a), the wing imaginal disc of *dLipin*-kd flies showed a significantly reduced number of PH3S10-positive cells in the wing margin and wing pouch (Figure 4d,g,j). Taken together with the increased cells in S phase, the reduced number of mitotic cells suggested that dysfunction of *dLipin* suppresses cell cycle transition from S to M phase in the wing imaginal disc, possibly owing to G2/M checkpoint activation.

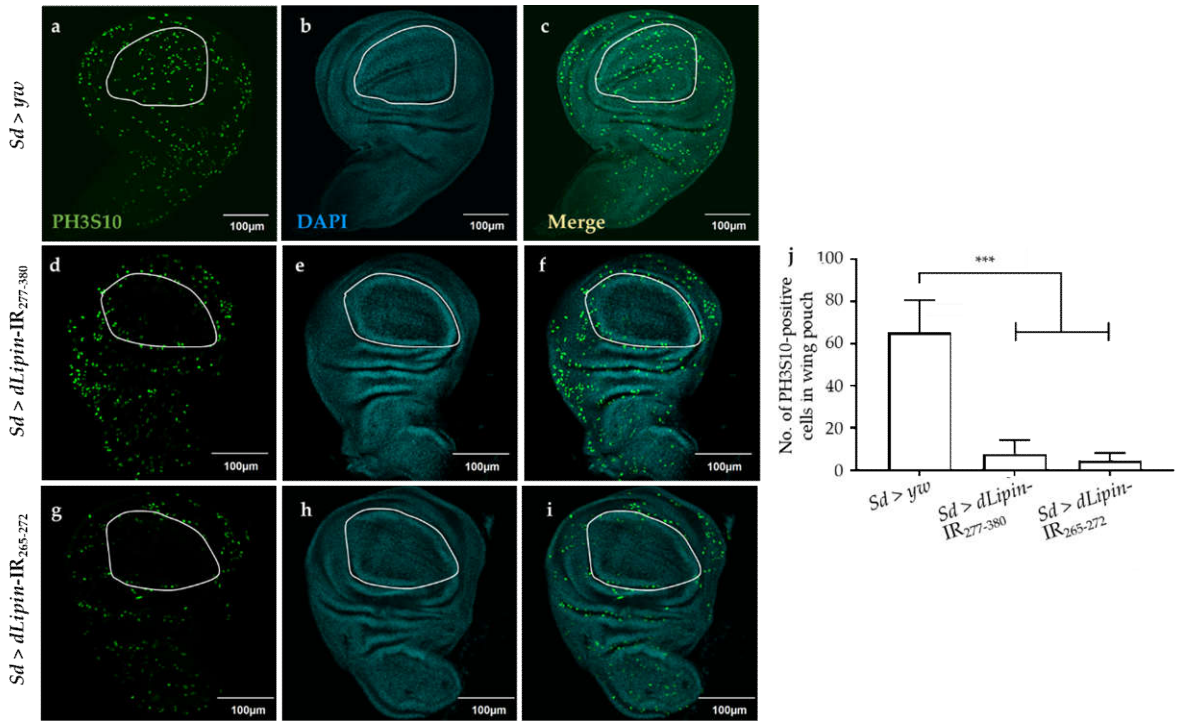

Figure 4. Knockdown of *dLipin* leads to a reduced number of mitotic cells in wing pouch. The wing imaginal discs from 3rd-instar larvae of control (*Sd* > *yw*) and *dLipin*-kd flies (*Sd* > *dLipin*-IR$_{265\text{-}272}$, *Sd* > *dLipin*-IR$_{277\text{-}380}$) were stained with DAPI to visualize the DNA (**b, e, h**) and anti-PH3S10 antibody followed by anti-rabbit IgG Alexa Fluor™ 488 antibody (**a, d, g**). Merged images of DAPI and PH3S10 antibody staining are shown (**c, f, i**). PH3S10-positive cells (mitotic cells)

in the wing pouch of 3rd-instar larvae were counted using MetaMorph software (n = 10 for each genotype) (**j**). Dotted line indicates the wing pouch of the wing imaginal disc. Data are expressed as the means ± S.D. The statistical significance of the difference between control and *dLipin*-kd flies was evaluated using one-way ANOVA. ***, $p < 0.01$; Scale bar, 100 μm; IR, inverted repeat. Genotypes: *Sd*-GAL4/+; +; + (**a**–**c**), *Sd*-GAL4/+; UAS-*dLipin*-IR$_{277\text{-}380}$/+; + (**d**–**f**), *Sd*-GAL4/+; UAS-*dLipin*-IR$_{265\text{-}272}$/+; + (**g**–**i**).

2.4. Dysfunction of dLipin Leads to Down-Regulated Expression of Cyclin B (CycB)

The CycB-CDK1 complex is necessary for the transition from G2 to M phase, and cyclin B expression peaks during late G2 and early mitosis [43–45]. We speculated that the G2/M checkpoint in *dLipin*-kd flies might be activated by dysregulated expression of cyclin B. To test this hypothesis, we checked the mRNA and protein levels of cyclin B in the wing imaginal discs of 3rd-instar larvae of the *dLipin*-kd strain by qRT-PCR and immunostaining with an anti-cyclin B antibody, respectively. As hypothesized, *CycB* mRNA was significantly reduced in both the knockdown flies (Figure 5j). Additionally, cyclin B protein level was decreased in the margin area of wing imaginal discs of *dLipin*-kd flies (Figure 5d,g), compared to that in the control flies (Figure 5a). These results suggested that the dysfunction of dLipin may lead to reduced expression of cyclin B and, subsequently, to activation of the G2/M checkpoint.

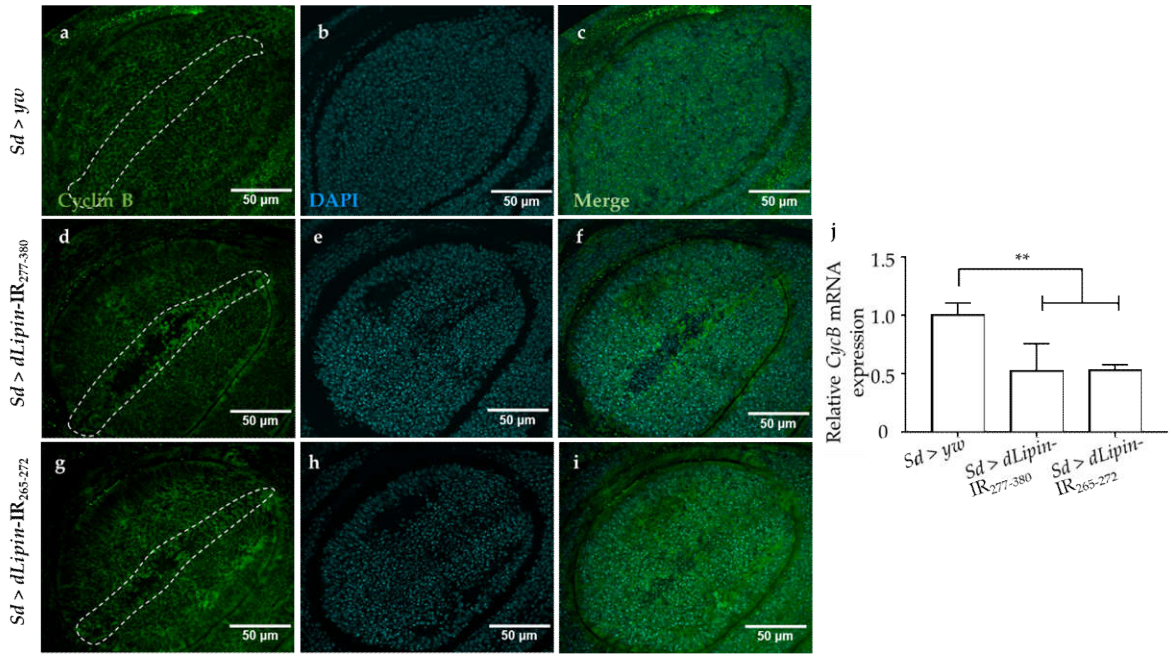

Figure 5. Induction of *dLipin* RNAi leads to reduced expression of the cyclin B in the wing margin area of wing imaginal discs. The wing imaginal discs were stained with DAPI to visualize the DNA (**b, e, h**) and mouse anti-cyclin B antibody followed by anti-mouse IgG Alexa Fluor™ 488 antibody (**a, d, g**). Merged images of DAPI and anti-cyclin B antibody (**c, f, i**). *CycB* mRNA levels in wing imaginal discs of 3rd-instar larvae of control and *dLipin*-kd flies were analyzed by RT-qPCR (n = 5 for each genotype). The relative *dLipin* mRNA level of *dLipin*-kd flies to that of control flies is shown (**j**). Data are expressed as the means ± S.D. The statistical significance of the difference between control and *dLipin*-kd flies was evaluated using one-way ANOVA. **, $p < 0.02$. The dotted lines indicate the margins of wing imaginal discs. Scale bar, 50 μm; IR, inverted repeat. Genotypes: *Sd*-GAL4/+; +; + (**a**–**c**), *Sd*-GAL4/+; UAS-*dLipin*-IR$_{277\text{-}380}$/+; + (**d**–**f**), *Sd*-GAL4/+; UAS-*dLipin*-IR$_{265\text{-}272}$/+; + (**g**–**i**).

2.5. Knockdown of dLipin Causes DNA Damage-Induced Apoptotic Cell Death

Activation of the G2/M checkpoint is known to prevent the cells from initiating mitosis when DNA damage occurs during G2, or when cells progress into G2 with some unrepaired damage inflicted during the previous S phase [46]. Upon DNA damage, both CycB transcription and protein level are down-regulated [47,48]. To clarify whether the activation of the G2/M checkpoint in *dLipin*-kd flies was

induced by DNA damage, we examined the expression of histone variant H2Av phosphorylated at Ser137 (γH2Av), the homolog of mammalian histone variant H2AX [49,50], which is a marker for an early signal of DNA damage induced by replication stress [51,52]. As shown in Figure 6d,g,j, *dLipin*-kd flies showed a markedly increased number of γH2Av-positive cells, indicating that the G2/M checkpoint was activated by DNA damage.

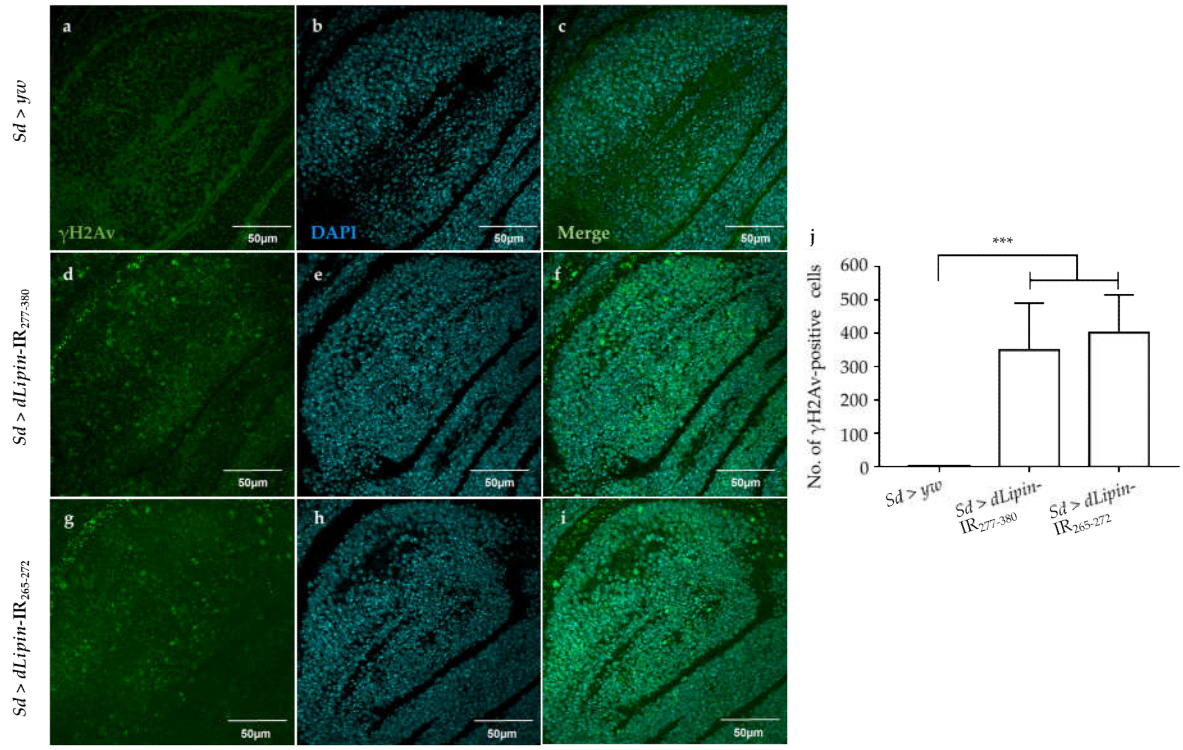

Figure 6. Knockdown of *dLipin* causes DNA damage in the wing pouch. Control and *dLipin*-kd wing imaginal discs were stained with DAPI to visualize the DNA (**b, e, h**) and mouse anti-γH2Av antibody followed by anti-mouse IgG Alexa Fluor™ 488 antibody (**a, d, g**). Merged images of DAPI and anti-γH2Av antibody staining (**c, f, i**). The number of γH2Av-positive cells in the wing pouch of imaginal discs of 3rd-instar larvae from control and *dLipin*-kd flies was analyzed using MetaMorph software (n = 14 for each genotype) (**j**). Data are expressed as the means ± S.D. The statistical significance of the difference between control and *dLipin*-kd flies was evaluated using one-way ANOVA. ***, $p < 0.01$. Scale bar, 50 μm; IR, inverted repeat. Genotypes: *Sd*-GAL4/+; +; + (**a–c**), *Sd*-GAL4/+; UAS-*dLipin*-IR$_{277\text{-}380}$/+; + (**d–f**), *Sd*-GAL4/+; UAS-*dLipin*-IR$_{265\text{-}272}$/+; + (**g–i**).

Next, we examined whether knockdown of *dLipin* enhanced apoptotic cell death following DNA damage. Upon immunostaining, *dLipin*-kd flies showed significantly increased cleaved caspase-3 signal in the wing pouch of wing imaginal discs (Figure 7d,g,j) in comparison to that in the controls (Figure 7a,j).

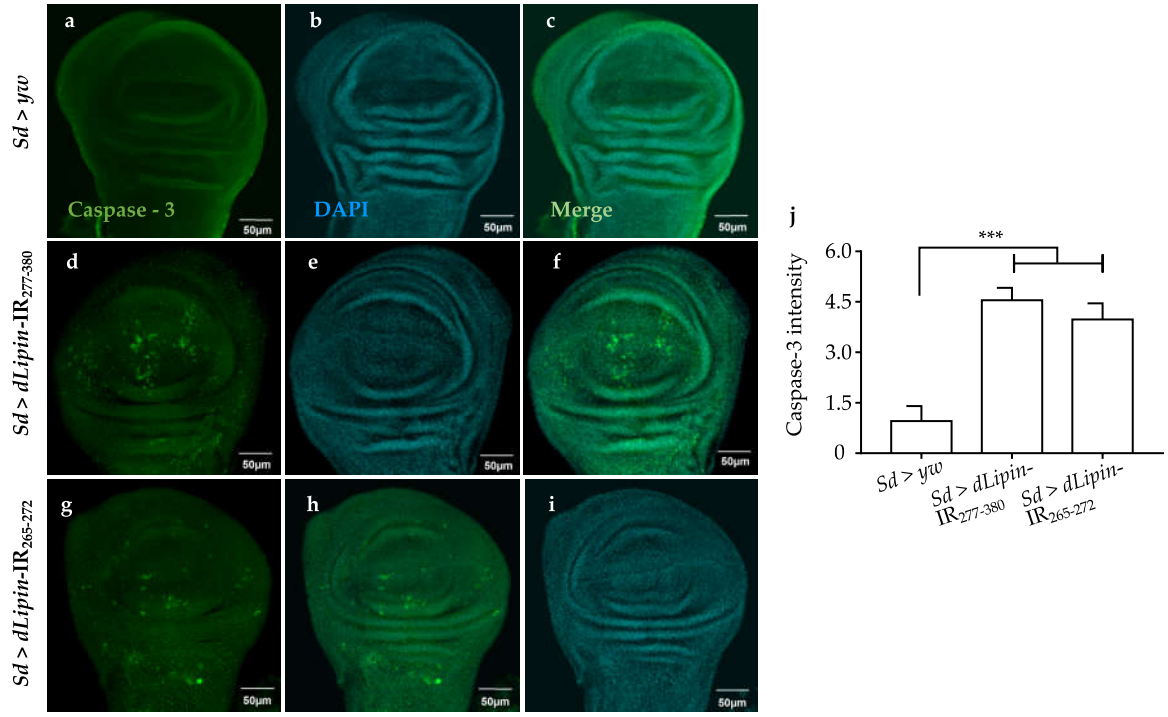

Figure 7. Knockdown of *dLipin* causes caspase-dependent cell death in wing imaginal discs of *Drosophila*. Wing imaginal discs from 3rd-instar larvae of control and *dLipin*-kd flies were stained with DAPI to visualize the DNA (**b, e, h**), and with rabbit anti-cleaved caspase-3 antibody followed by anti-rabbit IgG Alexa Fluor™ 488 antibody (**a, d, g**). Merged images of DAPI and anti-cleaved caspase-3 antibody are shown (**c, f, i**). The fluorescence intensity in the wing pouch stained with anti-cleaved caspase-3 antibody was analyzed using MetaMorph software (n = 14 for each genotype) (**j**). Data are expressed as the means ± S.D. The statistical significance of the difference between control and *dLipin*-kd flies was evaluated using one-way ANOVA. ***, $p < 0.01$; Scale bar, 50 μm. IR, inverted repeat. Genotypes: *Sd*-GAL4/+; +; + (**a**–**c**), *Sd*-GAL4/+; UAS-*dLipin*-IR$_{277\text{-}380}$/+; + (**d**–**f**), *Sd*-GAL4/+; UAS-*dLipin*-IR$_{254\text{-}476}$/+; + (**g**–**i**).

We analyzed the expression of the pro-apoptotic gene *reaper* (*rpr*) by using *dLipin*-kd flies that carry *rpr*-lacZ as a reporter. The results demonstrated that

dLipin knockdown in the margin area and wing pouch of wing imaginal disc, driven by *Sd*-GAL4, resulted in significantly up-regulated transcription of *rpr* (Figure 8d,g). In addition, we established *dLipin*-kd flies, in which death-associated inhibitor of apoptosis 1 (DIAP1) was overexpressed by the *Sd*-GAL4 driver, to examine whether the phenotype of *dLipin*-kd could be rescued. The *dLipin* knockdown phenotypes were partially rescued by *diap1* overexpression (Figure S4). The cleaved caspase-3 and anti-lacZ signals detected outside of the expression domain of *Sd*-GAL4 in Figures 7d,g and 8d,g could be explained by the non-cell autonomy. These results suggested that dysfunction of *dLipin* causes DNA damage-induced apoptotic cell death in the wing imaginal disc of *Drosophila*.

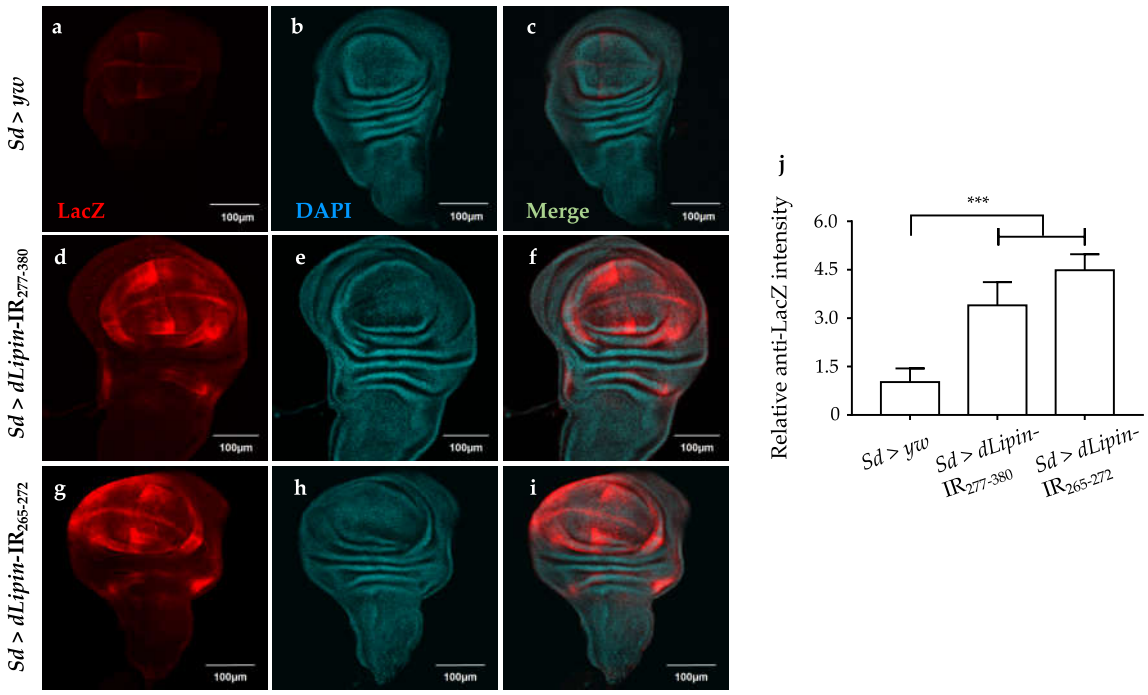

Figure 8. Knockdown of *dLipin* activates the pro-apoptotic gene *reaper*. Wing imaginal discs from the 3rd-instar larvae of control and *dLipin*-kd flies that carry *rpr*-lacZ were stained with an anti-lacZ antibody (**a, d, g**) and with DAPI (**b, e, h**). Both images were merged (**c, f, i**). The fluorescence intensities in the wing pouch stained with anti-lacZ were analyzed using MetaMorph software (n = 14 for each genotype) (**j**). Data are expressed as the means ± S.D. The statistical significance of the difference between control and *dLipin*-kd flies was evaluated using one-way

ANOVA. ***, $p < 0.01$; Scale bar, 100 μm; IR, inverted repeat. Genotypes: *Sd*-GAL4/+; +; *rpr*-lacZ/+ (**a**–**c**), *Sd*-GAL4/+; UAS-*dLipin*-IR$_{277\text{-}380}$/+; *rpr*-lacZ/+ (**d**–**f**), *Sd*-GAL4/+; UAS-*dLipin*-IR$_{254\text{-}476}$/+; *rpr*-lacZ/+ (**g**–**i**).

3. Discussion

Lipin reportedly has three main functions: As an enzyme catalyzing the production of DAG from PA, maintaining a balance between PA and DAG, and as an inducible transcriptional coactivator in conjunction with PPARγ to regulate several lipid metabolism-related genes [9,12]. Previous studies demonstrated that dLipin can be detected in wing imaginal discs [23], and is necessary for wing vein formation via BMP signaling [53]. However, there have been no reports regarding the functions of dLipin in wing blade formation. In the present study, we found that dLipin could be detected in the wing imaginal disc with a higher level in the margin of the wing pouch and the notum region, which become the wing margin and thorax of adult flies, compared to that in other areas. Knockdown of *dLipin* led to wing notching, down-curled wing, and significantly smaller wing size (Figure 2), suggesting the important role of dLipin in the normal formation of the wing blade. Furthermore, we showed that the abnormal formation of the wing in *dLipin*-kd flies is caused by the inhibition of the transition from S phase to M phase during the cell cycle.

A previous study demonstrated that mutation of dLipin induces reduced levels of TAG, which plays a central role in cellular lipid storage in invertebrates, in whole-larvae of *Drosophila* [23]. We hypothesized that knockdown of *dLipin* in the wing imaginal disc may affect the production of DAG from PA. Deficiency of DAG, which is a precursor to TAG, leads to deficient TAG content, thereby affecting the development of adult wing blades. However, our results of high-fat diet administration demonstrated that the curly and notched wings are not likely to be caused by the deficiency of TAG in wing imaginal discs of *dLipin*-kd flies (Figure 2). Dwyer et al. reported that PA and DAG are required for the biosynthesis of phospholipids [4], which are mainly found in cell membranes and

play pivotal roles in cell physiology [2,54]. Therefore, the deficiency of DAG may affect the cell cycle process, thereby disrupting wing formation. Moreover, lipin is a key regulator of nuclear membrane growth during the cell cycle in yeast [11]. Jackowski reported that phospholipids accumulated in the S phase [55], suggesting that the decrease in DAG by dLipin dysfunction may affect the cell cycle in S phase. Consistent with this, we found that *dLipin*-kd in the wing pouch of 3rd-instar larvae induced the accumulation of cells in S phase (Figure 3).

Laskye et al. showed that the entire DNA content in the nucleus must be completely and precisely replicated during the S phase of the cell cycle [56]. Earlier studies reported that phospholipids (i.e., cardiolipin, PA, phosphatidylglycerol, and phosphatidylinositol) inhibited DNA replication in mitochondria and the nucleus through interaction with DNA polymerases [7,57]. Notably, lipin can regulate the syntheses of phosphatidylcholine and other phospholipids by repressing key genes of the biosynthesis pathway in yeast [11]. It is; thus, possible that the increased PA in wing imaginal discs of *dLipin*-kd flies may inhibit the interaction between DNA polymerases and phospholipids, thereby causing DNA replication stress by generating incompletely replicated DNA.

The accumulation of cells in S phase in the wing margin of *dLipin*-kd wing imaginal discs might be associated with DNA damage induced by replication stress [58]. Moreover, our results showed that the wing margin and wing pouch of *dLipin*-kd wing imaginal discs exhibited increased expression of the γH2Av protein, a marker for DNA damage induced by replication stress (Figure 6). In addition, Ugrankar et al. reported that loss of *dLipin* in the fat body caused nuclei fragmentation [23]. Together, this evidence indicated that the accumulation of cells in S phase in the wing margin of 3rd-instar larvae of *dLipin*-kd strain was due to DNA damage in the cell cycle process.

The accuracy of DNA replication and division is facilitated by cell cycle DNA damage checkpoints [59,60], which are located at specific positions in the cell cycle to detect damage and allow sufficient time for DNA repair [34–36]. Our observations showed that the number of mitotic cells in M phase was significantly

reduced in the wing pouch of *dLipin*-kd flies (Figure 4). In addition, both transcription and protein levels of cyclin B were reduced in the wing imaginal disc of *dLipin*-kd flies, indicating activation of the G2/M checkpoint in these flies (Figure 5). We; therefore, concluded that the G2/M checkpoint was activated in response to DNA damage in these flies. It was also found that the cyclin B intensities of several cells located near the wing margin region of *dLipin*-kd flies were higher than those of the control. It is possible that elevation of the cyclin B level of neighboring cells may compensate for lack of cyclin B of cells in the wing margin of knockdown flies, although currently the mechanism underlying this response remains to be elucidated. There are four distinct pathways related to DNA damage response: transcriptional induction, cell cycle arrest (also known as DNA damage checkpoint), DNA repair, and apoptosis. These pathways work independently under certain conditions, but frequently interact to repair the damaged DNA or activate apoptosis [61–64]. We found increased signals of anti-cleaved caspase-3 antibody (Figure 7) and elevated expression of *reaper* gene (Figure 8) in the wing pouch of *dLipin*-kd flies. Taken together, these results implicated that dysfunction of *dLipin* might lead to apoptotic cell death induced by DNA damage in the wing imaginal disc of *Drosophila*.

In a state of starvation, dLipin in the fat tissue is translocated from the cytoplasm to the nucleus [23,24]. Lack of TORC1 leads to translocation of lipin-1 into the nucleus in mammalian cells [25]. In mouse, lipin-1 works as a transcriptional co-regulator and directly controls the gene encoding nuclear receptor PPARα, whereas lipin-1 overexpression causes the activation of genes related to fatty acid transport, ß-oxidation, the TCA cycle, and oxidative phosphorylation, including many target PPARα genes [11,65]. This suggests that lipin-1 directly regulates genes to overcome energy deficiency during starvation. However, we could not detect dLipin signals in the nucleus of wing imaginal disc cells in starvation conditions. In addition, it is as yet unclear what genes are regulated by nuclear dLipin in *Drosophila* and the mechanism thereof. Further studies are necessary to answer these questions. The translocation of mammalian

lipin-1 into the nucleus may affect gene expression through an unknown PAP-dependent mechanism that regulates nuclear levels of the transcription factor SREBP-1, which regulates the expression of genes related to lipid homeostasis [21]. Sethi et al. reported that SREBP-1 serves as a bridge between lipogenesis and cell cycle progression of clear cell renal carcinoma [66]. Thus, we could not exclude the possibility that *dLipin*-kd may indirectly inhibit SREBP-1 expression in the wing imaginal disc, thereby affecting cell cycle proliferation.

In conclusion, knockdown of *dLipin* in the wing imaginal disc of *Drosophila* causes DNA damage. The DNA damage activates the G2/M DNA damage checkpoint by regulating cyclin B expression, inhibiting the transition from S phase to M phase. Furthermore, *dLipin* dysfunction may lead to apoptosis of cells in the wing imaginal disc of *D. melanogaster*, leading to the formation of wing notching and a significantly smaller wing. This is the first report regarding the function of dLipin in wing development.

4. Materials and Methods

4.1. Fly Stocks

Fly stocks were maintained at 25 °C on standard food. Transgenic flies carrying UAS-*dLipin*-IR$_{265\text{-}272}$ and UAS-*dLipin*-IR$_{277\text{-}380}$ were obtained from the Bloomington Drosophila Stock Center (BDSC) and Vienna Drosophila Resource Center (VDRC), respectively. These flies carry an inverted repeat (IR) of the *lipin* gene (targeting regions from amino acid 265 to 272 and from 277 to 380, respectively) downstream of the UAS sequence, on the second chromosome. Target sequences for these two RNAi sequences were designed to have no off-target effects (VDRC and online dsCheck software http://dscheck.rnai.jp). All other flies used in this study were obtained from BDSC. The *yw* flies were used as the wild-type strain.

4.2. Staining

The wandering 3rd-instar larvae were dissected in PBS to collect wing imaginal discs. Approximately 20 to 30 wing imaginal discs were fixed in 4% formaldehyde

in PBS and reacted with antibodies as described previously [67]. Anti-dLipin antibody [20], provided kindly by Prof. Dr. Michael Lehmann (University of Arkansas, Arkansas, USA), was used at a 1:3000 dilution, and then anti-rabbit IgG Alexa Fluor™ 594 (Molecular Probes, Invitrogen, Carlsbad, CA, USA) was used at a dilution of 1:800. The wing imaginal discs were respectively treated with anti-histone H3 (phospho S10), anti-cleaved caspase-3 IgG, anti-LacZ (Cell Signaling Technology (CST), Tokyo, Japan), anti-cyclin B, and anti-γH2Av antibodies (Santa Cruz Biotechnology, Dallas, TX, USA) at a 1:600 dilution, followed by incubation with Alexa Fluor™ 488-conjugated anti-mouse IgG at a dilution of 1:800. For nuclei staining, 4',6-diamidino-2-phenylindole (DAPI; Molecular Probes, Eugene, OR, USA) was used.

Male and female transgenic fly were mated and kept for 1 day at 25 °C, then transferred to a new standard food tube for 1 h to deposit eggs to obtain a synchronized larval age. At the desired period of larval growth, wing imaginal discs were collected for assays. 5-Ethynyl-2′-deoxyuridine (EdU) labeling was performed according to the manufacturer's instructions (Molecular Probes).

After reacting with antibody, DAPI, or EdU, wing imaginal discs were mounted on a glass slide in Vectashield mounting medium (Vector Laboratories, Tokyo, Japan), and then inspected using a fluorescence FV10i microscope (Olympus, Tokyo, Japan). The fluorescence intensity in the wing pouch was analyzed using MetaMorph software (version 7.7.7.0; Molecular Devices, Sunnyvale, CA, USA), and the intensity in the wing pouch was subtracted from that of the area outside.

4.3. Starvation Assay

Pre-wandering 3rd-instar larvae of the *yw* strain were transferred to either standard food (fed larvae) or cotton plugs soaked in PBS (starved larvae). After 4 h, the wing imaginal discs were dissected out and reacted with anti-dLipin antibody as described above [24].

4.4. High-Fat Diet and Triglyceride Assays

The standard food supplement contained 0.8% agar (*w*/*v*), 9% cornmeal (*w*/*v*), 4% dry yeast (*w*/*v*), 0.05% (*w*/*v*) ethyl *p*-hydroxybenzoate, and 0.5% propionic acid

(*v*/*v*). For preparation of the high-fat diet, we added 20% (*w*/*v*) of food-grade coconut oil [68]. Five male and female transgenic flies were mated and allowed to lay eggs on the high-fat diet food for 2 days at 25 °C. The hatched larvae were grown on the same diet.

TAG contents were measured using the infinity triglycerides assay kit (Thermo Fisher Scientific, Waltham, MA, USA). Exactly 100 wing imaginal discs of wandering 3rd-instar larvae of each sample were dissected out and placed into tubes. The tubes were either placed on ice immediately for the assay, or stored at −80 °C for later assessment. Wing imaginal discs were homogenized in 100 μL of PBS containing 0.3 % Triton X-100. Homogenates were heated to 70 °C for 5 min, and then centrifuged at 16,150× *g* for 1 min at room temperature. The supernatant was transferred and centrifuged again at 30,050× *g* and 4 °C for 5 min. The final supernatant was assayed for TAG content. Briefly, 5 μL of supernatant was added to 200 μL of triglyceride reagent in the assay kit, and the mixture was incubated at 37 °C for 5 min. The optical density at 520 nm (OD_{520}) was measured, and TAG values were calculated according to the manufacturer's instructions by using glycerol standards for calibration.

4.5. Quantitative RT-PCR

Total RNA was extracted from 40 wing imaginal discs using standard Qiazol reagent (Qiagen, Hilden, Germany) followed by purification with the Qiagen RNeasy kit. cDNA was synthesized using the SimpliAmp™ Thermal Cycler (Life Technologies, Singapore, Singapore) according to the instruction manual. Quantitative polymerase chain reaction (PCR) was performed using the FastStart Essential DNA Green Master Mix (Roche, Mannheim, Germany) and a LightCycler 96 (Roche). *rp49* was used as an internal control. The sequences of gene-specific primers were as following: *dLipin*, forward: 5′-ATCCCACGTCCCTGATATCG-3′ and reverse: 5′-TTCATCTTGGTTGGTTAGCAGG-3′; for *CycB*, forward: 5′-GGATGCGGCACAGAAAGA-3′ and reverse: 5′-CTGTCCACCCGAGCTTTG-3′; for *rp49*, forward: 5′-ACCAGCTTCAAGATGACCATCC-3′ and reverse: 5′-

CTTGTTCGATCCGTAACCGATG-3′.

4.6. Statistical Analysis

The experiments were repeated at least three times. The data are expressed as means ± S.D. The statistical significance of differences was evaluated using a *t*-test and one-way ANOVA. The *p*-values of < 0.05 were considered significant.

5. Conclusions

Based on our results, we suggest that dLipin is necessary for the cell cycle progression subsequent to normal DNA replication during wing development of *D. melanogaster*. Further studies are required to understand the role of *dLipin* in the G2/M checkpoint and the expression of several genes implicated in DNA damage and repair. Moreover, a previous study demonstrated that the overexpression of *dLipin* in the Drosophila *dullard*, *ddd* hypomorphic mutant background rescues the atrophic wing vein phenotypes of the *ddd* mutant, indicating that the relationship between *dLipin* and *Dullard* is conserved in *Drosophila* [53]. Taken together, these results suggest that the balance of Lipin expression, which functions as an enzyme in the cytoplasm, is necessary for normal development of *D. melanogaster*.

6. References

1. Takeuchi, K.; Reue, K. Biochemistry, physiology, and genetics of GPAT, AGPAT, and lipin enzymes in triglyceride synthesis. *Am. J. Physiol. Endocrinol. Metab.* **2009**, *296*, E1195–E1209, doi:10.1152/ajpendo.90958.2008.
2. Lykidis, A.; Jackowski, S. Regulation of mammalian cell membrane biosynthesis. *Prog. Nucleic Acid Res. Mol. Biol.* **2001**, *65*, 361–393, doi:10.1016/S0079-6603(00)65010-9.
3. Wymann, M.P.; Schneiter, R. Lipid signalling in disease. *Nat. Rev. Mol. Cell Biol.* **2008**, *9*, 162–176, doi:10.1038/nrm2335.
4. Dwyer, J.R.; Donkor, J.; Zhang, P.; Csaki, L.S.; Vergnes, L.; Lee, J.M.; Dewald, J.; Brindley, D.N.; Atti, E.; Tetradis, S.; et al. Mouse lipin-1 and

lipin-2 cooperate to maintain glycerolipid homeostasis in liver and aging cerebellum. *Proc. Natl. Acad. Sci. USA* **2012**, *109*, E2486–E2495, doi:10.1073/pnas.1205221109.

5. Carman, G.M.; Han, G.-S. Phosphatidate phosphatase regulates membrane phospholipid synthesis via phosphatidylserine synthase. *Adv. Biol. Regul.* **2017**, doi:10.1016/j.jbior.2017.08.001.
6. Athenstaedt, K.; Daum, G. Phosphatidic acid, a key intermediate in lipid metabolism. *Eur. J. Biochem.* **1999**, *266*, 1–16, doi:10.1046/j.1432-1327.1999.00822.x.
7. Yoshida, S.; Tamiya-Koizumi, K.; Kojima, K. Interaction of DNA polymerases with phospholipids. *Biochim. Biophys. Acta* **1989**, *1007*, 61–66, doi:10.1016/0167-4781(89)90130-9.
8. Harris, T.E.; Finck, B.N. Dual function lipin proteins and glycerolipid metabolism. *Trends Endocrinol. Metab.* **2011**, *22*, 226–233, doi:10.1016/j.tem.2011.02.006.
9. Ahmadian, M.; Duncan, R.E.; Jaworski, K.; Sarkadi-Nagy, E.; Sul, H.S. Triacylglycerol metabolism in adipose tissue. *Future Lipidol.* **2007**, *2*, 229–237, doi:10.2217/17460875.2.2.229.
10. Coleman, R.A.; Lee, D.P. Enzymes of triacylglycerol synthesis and their regulation. *Prog. Lipid Res.* **2004**, *43*, 134–176, doi:10.1016/S0163-7827(03)00051-1.
11. Santos-Rosa, H.; Leung, J.; Grimsey, N.; Peak-Chew, S.; Siniossoglou, S. The yeast lipin Smp2 couples phospholipid biosynthesis to nuclear membrane growth. *EMBO J.* **2005**, *24*, 1931–1941, doi:10.1038/sj.emboj.7600672.
12. Lin, J.; Handschin, C.; Spiegelman, B.M. Metabolic control through the PGC-1 family of transcription coactivators. *Cell Metab.* **2005**, *1*, 361–370, doi:10.1016/j.cmet.2005.05.004.
13. Grimsey, N.; Han, G.S.; O'Hara, L.; Rochford, J.J.; Carman, G.M.; Siniossoglou, S. Temporal and spatial regulation of the phosphatidate

phosphatases lipin 1 and 2. *J. Biol. Chem.* **2008**, *283*, 29166–29174, doi:10.1074/jbc.M804278200.

14. Peterfy, M.; Phan, J.; Xu, P.; Reue, K. Lipodystrophy in the fld mouse results from mutation of a new gene encoding a nuclear protein, lipin. *Nat. Genet.* **2001**, *27*, 121–124, doi:10.1038/83685.
15. Reue, K.; Brindley, D.N. Thematic Review Series: Glycerolipids. Multiple roles for lipins/phosphatidate phosphatase enzymes in lipid metabolism. *J. Lipid Res.* **2008**, *49*, 2493–2503, doi:10.1194/jlr.R800019-JLR200.
16. Harris, T.E.; Huffman, T.A.; Chi, A.; Shabanowitz, J.; Hunt, D.F.; Kumar, A.; Lawrence, J.C.J. Insulin controls subcellular localization and multisite phosphorylation of the phosphatidic acid phosphatase, lipin 1. *J. Biol. Chem.* **2007**, *282*, 277–286, doi:10.1074/jbc.M609537200.
17. Donkor, J.; Sariahmetoglu, M.; Dewald, J.; Brindley, D.N.; Reue, K. Three mammalian lipins act as phosphatidate phosphatases with distinct tissue expression patterns. *J. Biol. Chem.* **2007**, *282*, 3450–3457, doi:10.1074/jbc.M610745200.
18. Gropler, M.C.; Harris, T.E.; Hall, A.M.; Wolins, N.E.; Gross, R.W.; Han, X.; Chen, Z.; Finck, B.N. Lipin 2 Is a Liver-enriched Phosphatidate Phosphohydrolase Enzyme That is Dynamically Regulated by Fasting and Obesity in Mice. *J. Biol. Chem.* **2009**, *284*, 6763–6772, doi:10.1074/jbc.M807882200.
19. Joseleau-Petit, D.; Kepes, F.; Peutat, L.; D'Ari, R.; Kepes, A. DNA replication initiation, doubling of rate of phospholipid synthesis, and cell division in Escherichia coli. *J. Bacteriol.* **1987**, *169*, 3701–3706, doi:10.1128/jb.169.8.3701-3706.1987.
20. Tange, Y.; Hirata, A.; Niwa, O. An evolutionarily conserved fission yeast protein, Ned1, implicated in normal nuclear morphology and chromosome stability, interacts with Dis3, Pim1/RCC1 and an essential nucleoporin. *J. Cell Sci.* **2002**, *115*, 4375–4385, doi:10.1242/jcs.00135.
21. Reue, K. The lipin family: Mutations and metabolism. *Curr. Opin. Lipidol.*

2009, *20*, 165–170, doi:10.1097/MOL.0b013e32832adee5.

22. Phan, J.; Reue, K. Lipin, a lipodystrophy and obesity gene. *Cell Metab.* **2005**, *1*, 73–83, doi:10.1016/j.cmet.2004.12.002.
23. Ugrankar, R.; Liu, Y.; Provaznik, J.; Schmitt, S.; Lehmann, M. Lipin is a central regulator of adipose tissue development and function in Drosophila melanogaster. *Mol. Cell. Biol.* **2011**, *31*, 1646–1656, doi:10.1128/MCB.01335-10.
24. Schmitt, S.; Ugrankar, R.; Greene, S.E.; Prajapati, M.; Lehmann, M. Drosophila Lipin interacts with insulin and TOR signaling pathways in the control of growth and lipid metabolism. *J. Cell Sci.* **2015**, *128*, 4395–4406, doi:10.1242/jcs.173740.
25. Peterson, T.R.; Sengupta, S.S.; Harris, T.E.; Carmack, A.E.; Kang, S.A.; Balderas, E.; Guertin, D.A.; Madden, K.L.; Carpenter, A.E.; Finck, B.N.; et al. mTOR complex 1 regulates lipin 1 localization to control the SREBP pathway. *Cell* **2011**, *146*, 408–420, doi:10.1016/j.cell.2011.06.034.
26. Nigg, E.A. Cyclin-dependent protein kinases: Key regulators of the eukaryotic cell cycle. *Bioessays* **1995**, *17*, 471–480, doi:10.1002/bies.950170603.
27. Yang, V.W. The Cell Cycle. In *Physiology of the Gastrointestinal Tract*, 5th ed.; Johnson, L.R., Ghishan, F.K., Kaunitz, J.D., Merchant, J.L., Said, H.M., Wood, J.D.B.T.-P., Eds.; Academic Press: Boston, MA, USA, 2012; Chapter 15, pp. 451–471. ISBN 978-0-12-382026-6.
28. Morgan, D.O. Cyclin-dependent kinases: Engines, clocks, and microprocessors. *Annu. Rev. Cell Dev. Biol.* **1997**, *13*, 261–291, doi:10.1146/annurev.cellbio.13.1.261.
29. Edgar, B.A.; Lehman, D.A.; O'Farrell, P.H. Transcriptional regulation of string (cdc25): A link between developmental programming and the cell cycle. *Development* **1994**, *120*, 3131–3143.
30. Edgar, B.A.; O'Farrell, P.H. Genetic control of cell division patterns in the Drosophila embryo. *Cell* **1989**, *57*, 177–187.

31. Cobrinik, D. Pocket proteins and cell cycle control. *Oncogene* **2005**, *24*, 2796–2809, doi:10.1038/sj.onc.1208619.
32. Chow, K.N.; Starostik, P.; Dean, D.C. The Rb family contains a conserved cyclin-dependent-kinase-regulated transcriptional repressor motif. *Mol. Cell. Biol.* **1996**, *16*, 7173–7181, doi:10.1128/mcb.16.12.7173.
33. Harbour, J.W.; Luo, R.X.; Dei Santi, A.; Postigo, A.A.; Dean, D.C. Cdk phosphorylation triggers sequential intramolecular interactions that progressively block Rb functions as cells move through G1. *Cell* **1999**, *98*, 859–869, doi:10.1016/S0092-8674(00)81519-6.
34. Elledge, S.J. Cell cycle checkpoints: Preventing an identity crisis. *Science* **1996**, *274*, 1664–1672, doi:10.1126/science.274.5293.1664.
35. Murray, A. Cell cycle checkpoints. *Curr. Opin. Cell Biol.* **1994**, *6*, 872–876, doi:10.1016/0955-0674(94)90059-0.
36. Pietenpol, J.A.; Stewart, Z.A. Cell cycle checkpoint signaling: Cell cycle arrest versus apoptosis. *Toxicology* **2002**, *181–182*, 475–481, doi:10.1016/S0300-483X(02)00460-2.
37. Brand, A.H.; Perrimon, N. Targeted gene expression as a means of altering cell fates and generating dominant phenotypes. *Development* **1993**, *118*, 401–415.
38. Guss, K.A.; Benson, M.; Gubitosi, N.; Brondell, K.; Broadie, K.; Skeath, J.B. Expression and function of scalloped during Drosophila development. *Dev. Dyn.* **2013**, *242*, 874–885, doi:10.1002/dvdy.23942.
39. Wessells, R.J.; Grumbling, G.; Donaldson, T.; Wang, S.H.; Simcox, A. Tissue-specific regulation of vein/EGF receptor signaling in Drosophila. *Dev. Biol.* **1999**, *216*, 243–259, doi:10.1006/dbio.1999.9459.
40. Salic, A.; Mitchison, T.J. A chemical method for fast and sensitive detection of DNA synthesis in vivo. *Proc. Natl. Acad. Sci. USA* **2008**, *105*, 2415–2420, doi:10.1073/pnas.0712168105.
41. Hsu, J.Y.; Sun, Z.W.; Li, X.; Reuben, M.; Tatchell, K.; Bishop, D.K.; Grushcow, J.M.; Brame, C.J.; Caldwell, J.A.; Hunt, D.F.; et al. Mitotic

phosphorylation of histone H3 is governed by Ipl1/aurora kinase and Glc7/PP1 phosphatase in budding yeast and nematodes. *Cell* **2000**, *102*, 279–291, doi:10.1016/S0092-8674(00)00034-9.

42. Wei, Y.; Yu, L.; Bowen, J.; Gorovsky, M.A.; Allis, C.D. Phosphorylation of histone H3 is required for proper chromosome condensation and segregation. *Cell* **1999**, *97*, 99–109, doi:10.1016/S0092-8674(00)80718-7.
43. Kastan, M.B.; Bartek, J. Cell-cycle checkpoints and cancer. *Nature* **2004**, *432*, 316–323, doi:10.1038/nature03097.
44. Lindqvist, A.; Rodriguez-Bravo, V.; Medema, R.H. The decision to enter mitosis: Feedback and redundancy in the mitotic entry network. *J. Cell Biol.* **2009**, *185*, 193–202, doi:10.1083/jcb.200812045.
45. Darzynkiewicz, Z.; Gong, J.; Juan, G.; Ardelt, B.; Traganos, F. Cytometry of cyclin proteins. *Cytometry* **1996**, *25*, 1–13, doi:10.1002/(SICI)1097-0320(19960901)25:1<1::AID-CYTO1>3.0.CO;2-N.
46. Wang, J.Y.J.; Cho, S.K. Coordination of Repair, Checkpoint, and Cell Death Responses to DNA Damage. In *DNA Repair and Replication*; Wei Yang, Ed.; Academic Press: Boston, MA, USA, 2004; Volume 69, pp. 101–135. ISBN 0065-3233.
47. Maity, A.; McKenna, W.G.; Muschel, R.J. Evidence for post-transcriptional regulation of cyclin B1 mRNA in the cell cycle and following irradiation in HeLa cells. *EMBO J.* **1995**, *14*, 603–609, doi:10.1002/j.1460-2075.1995.tb07036.x.
48. Maity, A.; Hwang, A.; Janss, A.; Phillips, P.; McKenna, W.G.; Muschel, R.J. Delayed cyclin B1 expression during the G2 arrest following DNA damage. *Oncogene* **1996**, *13*, 1647–1657.
49. Peng, J.C.; Karpen, G.H. Heterochromatic genome stability requires regulators of histone H3 K9 methylation. *PLoS Genet.* **2009**, *5*, e1000435, doi:10.1371/journal.pgen.1000435.
50. Madigan, J.P.; Chotkowski, H.L.; Glaser, R.L. DNA double-strand break-induced phosphorylation of Drosophila histone variant H2Av helps

prevent radiation-induced apoptosis. *Nucleic Acids Res.* **2002**, *30*, 3698–3705, doi:10.1093/nar/gkf496.

51. Sharma, A.; Singh, K.; Almasan, A. Histone H2AX phosphorylation: A marker for DNA damage. *Methods Mol. Biol.* **2012**, *920*, 613–626, doi:10.1007/978-1-61779-998-3_40.
52. Kuo, L.J.; Yang, L.X. Gamma-H2AX-a novel biomarker for DNA double-strand breaks. *In Vivo* **2008**, *22*, 305–309.
53. Liu, Z.; Matsuoka, S.; Enoki, A.; Yamamoto, T.; Furukawa, K.; Yamasaki, Y.; Nishida, Y.; Sugiyama, S. Negative modulation of bone morphogenetic protein signaling by Dullard during wing vein formation in Drosophila. *Dev. Growth Differ.* **2011**, *53*, 822–841, doi:10.1111/j.1440-169X.2011.01289.x.
54. Van Meer, G.; Voelker, D.R.; Feigenson, G.W. Membrane lipids: Where they are and how they behave. *Nat. Rev. Mol. Cell Biol.* **2008**, *9*, 112–124, doi:10.1038/nrm2330.
55. Jackowski, S. Coordination of membrane phospholipid synthesis with the cell cycle. *J. Biol. Chem.* **1994**, *269*, 3858–3867.
56. Laskey, R.A.; Fairman, M.P.; Blow, J.J. S phase of the cell cycle. *Science* **1989**, *246*, 609–614, doi:10.1126/science.2683076.
57. Shoji-Kawaguchi, M.; Izuta, S.; Tamiya-Koizumi, K.; Suzuki, M.; Yoshida, S. Selective Inhibition of DNA Polymerase a by Phosphatidylinositol. *J. Biochem.* **1995**, *117*, 1095–1099, doi:10.1093/oxfordjournals.jbchem.a124812.
58. Yang, V.W. The Cell Cycle. *Physiol. Gastrointest. Tract* **2012**, 451–471, doi:10.1016/B978-0-12-382026-6.00015-4.
59. Senderowicz, A.M.; Sausville, E.A. Preclinical and clinical development of cyclin-dependent kinase modulators. *J. Natl. Cancer Inst.* **2000**, *92*, 376–387, doi:10.1093/jnci/92.5.376.
60. Sherr, C.J. The Pezcoller Lecture: Cancer cell cycles revisited. *Cancer Res.* **2000**, *60*, 3689–3695.

61. Sancar, A.; Lindsey-Boltz, L.A.; Unsal-Kacmaz, K.; Linn, S. Molecular mechanisms of mammalian DNA repair and the DNA damage checkpoints. *Annu. Rev. Biochem.* **2004**, *73*, 39–85, doi:10.1146/annurev.biochem.73.011303.073723.
62. Zhou, B.B.; Elledge, S.J. The DNA damage response: Putting checkpoints in perspective. *Nature* **2000**, *408*, 433–439, doi:10.1038/35044005.
63. Song, Y.-H. Drosophila melanogaster: A model for the study of DNA damage checkpoint response. *Mol. Cells* **2005**, *19*, 167–179, doi:10.1360/gs050205.
64. Harper, J.W.; Elledge, S.J. The DNA damage response: Ten years after. *Mol. Cell* **2007**, *28*, 739–745, doi:10.1016/j.molcel.2007.11.015.
65. Finck, B.N.; Gropler, M.C.; Chen, Z.; Leone, T.C.; Croce, M.A.; Harris, T.E.; Lawrence, J.C.J.; Kelly, D.P. Lipin 1 is an inducible amplifier of the hepatic PGC-1alpha/PPARalpha regulatory pathway. *Cell Metab.* **2006**, *4*, 199–210, doi:10.1016/j.cmet.2006.08.005.
66. Sethi, G.; Shanmugam, M.K.; Kumar, A.P. SREBP-1c as a molecular bridge between lipogenesis and cell cycle progression of clear cell renal carcinoma. *Biosci. Rep.* **2017**, *37*, doi:10.1042/BSR20171270.
67. Men, T.T.; Binh, T.D.; Yamaguchi, M.; Huy, N.T.; Kamei, K. Function of Lipid Storage Droplet 1 (Lsd1) in Wing Development of Drosophila melanogaster. *Int. J. Mol. Sci.* **2016**, *17*, doi:10.3390/ijms17050648.
68. Heinrichsen, E.T.; Haddad, G.G. Role of high-fat diet in stress response of Drosophila. *PLoS ONE* **2012**, *7*, e42587, doi:10.1371/journal.pone.0042587.

Chapter 2. Role of Serotonin Transporter in Eye Development of *Drosophila melanogaster*

1. Introduction

The serotonergic system is conserved from insects to mammals, and it plays a pivotal role in the mental health of organisms [1,2]. The serotonergic system exists in both the brain and peripheral organs. In the brain, serotonin (5-hydroxytryptamine, 5-HT), the core molecule of the system, acts as a neurotransmitter and is associated with the feeling of wellness and happiness [3]. Altered regulation of serotonin concentration in the brain has been recorded not only in a vast range of behavioral functions, such as wake/sleep states, appetite, and sexual behavior, but also in the causation of multiple severe psychotic disorders, such as depression, bipolar disorder, and schizophrenia [4,5]. Although the roles of serotonin in the brain have been intensively investigated, the serotonergic function in peripheral organs, where serotonin acts as a hormonal molecule, is mostly uninvestigated, even though 95% of the serotonin in the whole body is produced by the gastrointestinal tract [6]. One of the essential components in the regulation of serotonin is serotonin transporter (SerT) or 5-hydroxytryptamine transporter (5-HTT), which is a monoamine transporter protein responsible for the reuptake of serotonin into neurons after synaptic transmission in mammals [7]. SerT is a transmembrane transporter that is highly conserved in various organisms from insects to mammals. SerT in the central nervous system is associated with anxiety and depression-related psychological conditions, thereby making it a target for a large number of antidepressant drugs called selective serotonin reuptake inhibitors (SSRIs) [8]. On the other hand, peripheral SerT has been reported to play significant roles in cardiovascular processes, appetite regulation, endocrine mediation, and reproduction [9–12]. Still, the function of SerT in developmental processes is poorly understood.

Drosophila melanogaster is a versatile model organism for researching various biological and physiological mechanisms [13]. The compound eye of an adult fly is composed of approximately 750 unit eyes, known as ommatidia. Each

ommatidium consists of a core of eight photoreceptor neurons, R1–R8. *Drosophila* compound eyes are derived from the eye-antennal disc. In the eye disc of *Drosophila* third-instar larva, the morphogenetic furrow (MF) represents the mitotic wave of cells, which sweeps from posterior to anterior. The cells exiting just ahead of MF in the anterior area and within the MF will undergo cell cycle arrest in the synchronized G1 phase, waiting for their fate to be determined, and form a progenitor cell pool. As MF propagates, the progenitor cells are recruited into photoreceptor pre-clusters and specified as several types of photoreceptor neurons (R8, R2, R5, R3, or R4). In cells just at the back of MF in the posterior area, which have not started to differentiate, one more round of division called the second mitotic wave (SMW) occurs to recruit cells into other types of photoreceptor neurons (R1, R6, or R7) [14–16]. In the posterior region, after the SMW passes, no additional cell cycles occur within the larval disc. Because there are more cells than needed in the eye disc to form ~750 ommatidia, undifferentiated cells will either later differentiate into photoreceptors or accessory cells, or be removed via apoptosis during pupation [17]. Since the core of photoreceptor neurons is arrayed in a structure that is accurately repetitive in healthy individuals [18], small abnormalities in the compound eyes can be easily observed, which make compound eye tissues ideal for examining cell fate via signaling transduction pathways. Thus, we chose the *Drosophila* compound eye as target tissues for investigating the role of SerT in the eye development.

Drosophila and mammals share a highly conserved phosphatidylinositol 3-kinase (PI3K)/Akt signaling pathway, which plays a vital role in regulating cellular growth and energy metabolism [19,20]. Moreover, multiple pieces of evidence showed the relation between this pathway and the development of the *Drosophila* compound eye. Palomero et al. (2007) showed the interaction of PTEN or Akt with Notch results in abnormal eye growth and tumorigenesis [21]. The target of rapamycin (TOR) is also involved in eye development, as TOR directly couples with the adaptor protein Unk. Bateman, J.M. [22] showed that together, TOR and Unk mediate the differentiation fate of photoreceptors R1, R6 and R7. Moreover,

the activity of the TOR complexes are required for hyperplasia upon elevated PI3K signaling in the compound eye [23]. Slade and Staveley (2015) showed that numerous novel Akt1 mutants exhibit fewer ommatidia with reduced size [24]. We hypothesized that the PI3K/Akt pathway mediates the role of SerT in the development of the compound eye in *Drosophila melanogaster*.

2. Results

2.1. SerT Knockdown Disrupts Healthy Eye Development

Despite multiple studies that explore SerT expression in the central nervous system of *Drosophila* [25,26], there is no evidence of SerT expression in the imaginal eye discs. In this research, SerT expression was visualized by a specific antibody for *Drosophila* SerT. Anti-SerT signals were distributed outside of the nucleus throughout the eye imaginal disc, showing high intensity (Figure 1B,B').

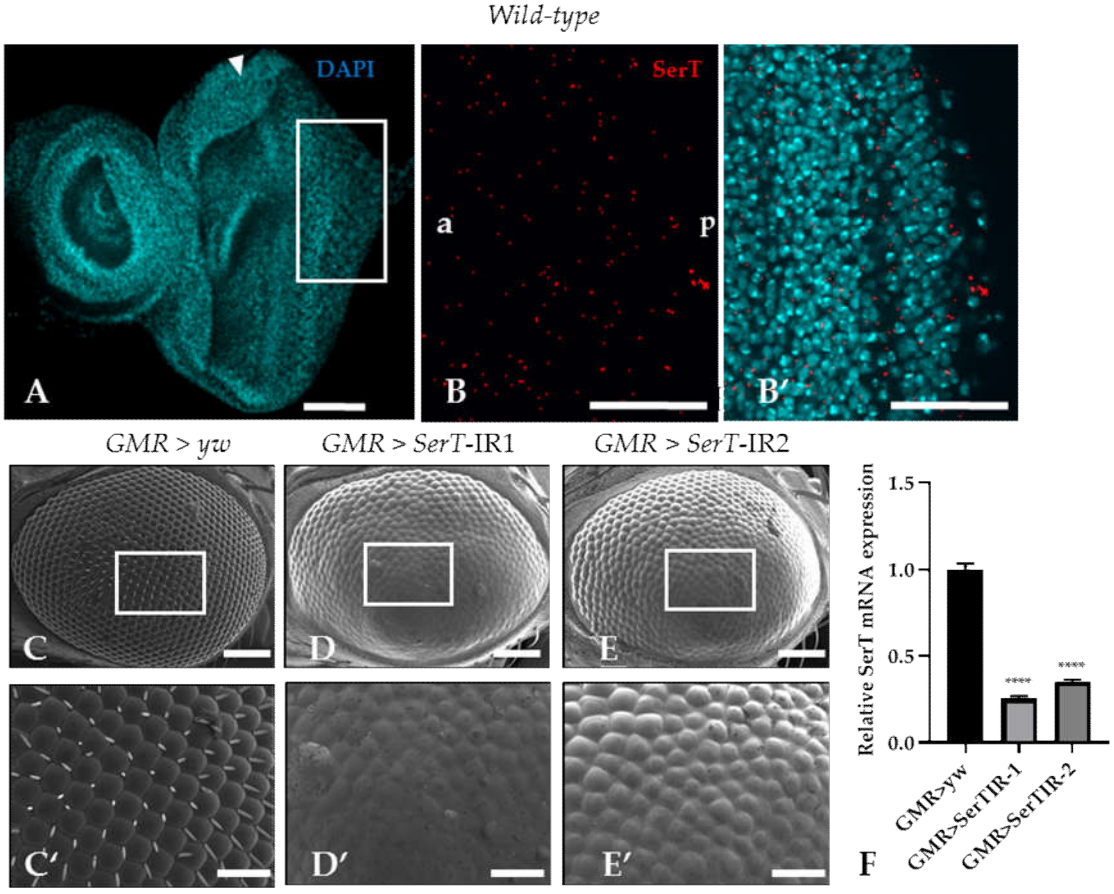

Figure 1. *SerT* knockdown induces a rough phenotype in the adult compound eye. The eye imaginal discs of wild-type third instar larvae were stained with

4′,6-diamidino-2-phenylindole (DAPI) to visualize the nucleus (**A**). The posterior region in the box stained with rabbit anti-*Drosophila* SerT antibody followed by anti-rabbit IgG Alexa Fluor™ 594 antibody was used for detecting SerT (**B**), and the merged image is shown (**B'**). The images are representative of 10 eye imaginal discs. Scanning electron micrographs of the compound eyes of flies carrying *GMR*-Gal4/*yw*; +; + (**C**), *GMR*-Gal4/Y; UAS-*SerT*-IR1/+; +, (**D**), *GMR*-Gal4/Y; and UAS-*SerT*-IR2/+; + (**E**). Larger images of the boxed regions are also shown (**C'**–**E'**). Phenotypes were observed independently in at least three individuals of each fly lines, and no significant change was found in three individuals of the same line. Relative mRNA expression of *SerT* gene in eye discs of flies contains *GMR* > *yw*, *GMR* > *SerT*IR-1, and *GMR* > *SerT*IR-2, $n = 5$ (**F**). Scale bars indicate 100 μm (**A**,**B**,**B'**,**C**–**E**) and 30 μm (**C'**–**E'**). The triangles indicate MF. a, anterior; p, posterior; **** $p < 0.0001$

Then, to determine the role of SerT in eye development, we investigated the effect of the reduction of SerT protein in the compound eye by using a GAL4/Upstream activation sequence (GAL4/UAS) system. Two *UAS-SerT* RNAi strains that have different inverted repeat sequences downstream of the *UAS* sequence with no overlap were used to exclude the possibility of off-target knockdown. The *UAS-SerT* RNAi strains were crossed with the *GMR*-GAL4 driver that expresses GAL4 in the eye under the control of glass enhancer; therefore, the offspring strongly expressed *SerT* RNAi in all the cells behind the MF, causing its specific knockdown in the eye. The knockdown strains, *GMR* > *SerT*-inverted repeat (IR)1 (Figure 1D,D') and *GMR* > *SerT*-IR2 (Figure 1E,E'), showed a rough phenotype in 100% of the adult compound eyes, in which the ommatidia were oddly shaped, and the bristles were lost. As the *GMR* > *SerT*-IR1 strain expressed a more severe phenotype, we chose this strain for further experiments. These data suggested that SerT played an important role in the development of the compound eye.

2.2. SerT Knockdown Induces Cell Death Via a Caspase-Dependent Pathway

Previous reports suggested that the rough eye phenotype may be caused by excessive cell death [27,28]. Thus, we stained the eye disc of third-instar larvae with anti-caspase-3 antibody. The number of the caspase-3-positive signal was significantly higher (4.4-fold) in knockdown flies (*SerT*-kd) than in wild-type flies, suggesting an increase in caspase-dependent cell death (Figure 2A,A'). This result was further confirmed by introducing either the *p35* or *diap1* gene, both of which encoded apoptosis inhibitors, into knockdown flies. The flies carrying *UAS-p35* or *UAS-diap1* in the background of *SerT* knockdown showed less a severe phenotype (Figure 2D–D",E–E"). The ommatidia structures slightly recovered, and the bristles were partially regenerated. Although flies carrying *UAS-gfp* and *SerT*-IR, which were generated as control, showed no significant rescue compared with the knockdown flies (Figure 2C–C").

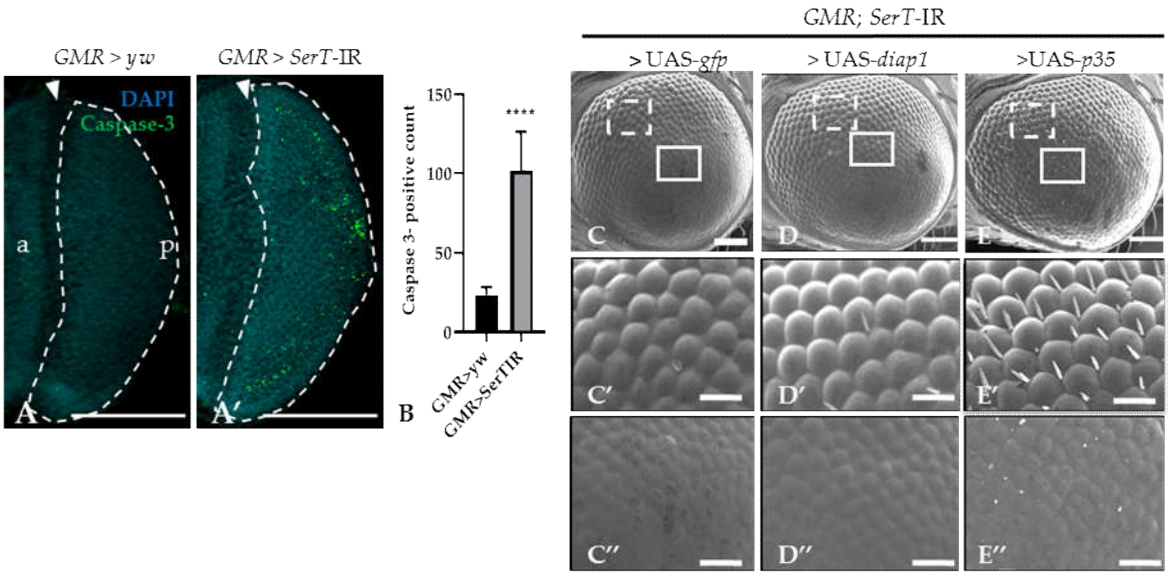

Figure 2. *SerT* knockdown induces caspase-dependent cell death. Region posterior to the morphogenetic furrow (MF) in the eye discs of third-instar larvae carrying *GMR > yw* as a control (**A**) and *GMR > SerT-IR* as *SerT*-kd (**A'**) were stained with anti-caspase-3 antibody followed by secondary antibodies labeled with Alexa488. Quantification of caspase-3 positive signal count in the posterior region surrounded by dotted lines (**B**). Scanning electron micrograph of adult compound

eyes of flies carrying *GMR-Gal4/Y, SerT-IR*/UAS-*gfp, +* (**C**), *GMR-Gal4/Y, SerT-IR*/UAS-*diap1*, + (**D**), and *GMR-Gal4/Y, SerT-IR*/UAS-*p35, +* (**E**). Larger images of the boxed regions with dotted white line and solid white line in (**C**–**E**) are shown in (**C'**–**E'**,**C"**–**E"**), respectively. Scale bar indicates 100 (**A**,**A'**,**C**–**E**) and 30 µm (**C'**–**E'**,**C"**–**E"**). The triangles point to the MF. a, anterior; p, posterior; ****, $p < 0.0001$.

2.3. SerT Knockdown Increases the Number of Cells in S-Phase in the Eye Imaginal Discs

Given the increased level of cell death, we hypothesized that *SerT*-kd might cause cell cycle defects in the eye imaginal discs. To prove this hypothesis, we utilized the 5-ethynyl-2′deoxyuridine (EdU) incorporation assay, which can detect proliferating S-phase cells. The result showed that there was a significant increase (2.4-fold) in the number of EdU-positive cells in the posterior area of *SerT*-kd flies than in that of control flies (the region surrounded by dotted lines in Figure 3A,A'). Moreover, the inhibition of apoptosis by the expression of DIAP1 significantly decreased the number of S-phase cells (Figure 3A"), suggesting a link between two phenomena. Moreover, we also detected the abnormal organization of cone cell nuclei by DAPI staining, which might be a result of excessive proliferation (Figure 3C,C'). On the other hand, we found that there was no change in the number of cells in the M-phase, as determined by anti-phosphorylated histone 3 antibody, between *SerT*-kd and control flies (Figure 3D,D',E). This suggests that only the number of cells in S-phase was affected, whereas the process of cell proliferation was not. In addition, we eliminated the possibility of DNA-damage causing excessive proliferation or cell death by staining the posterior eye disc with anti-phosphorylated-gamma-histone 2A, a known DNA-damage marker [29]. Low-signal intensity was observed in both the control and *SerT*-kd (Figure 3F,F',G), suggesting that DNA-damage did not cause the phenotype.

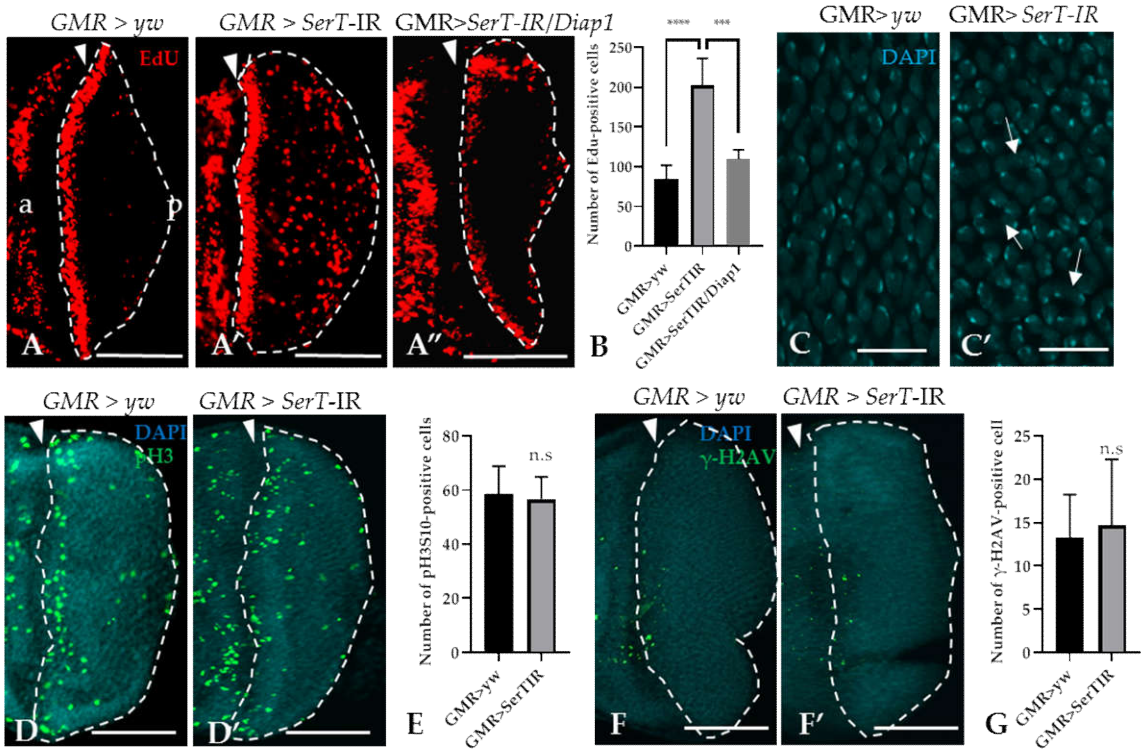

Figure 3. Knockdown of *SerT* induces a high accumulation of cells in the S-phase, but not in the M-phase. The region posterior to the MF stained with EdU in third instar larvae carrying *GMR* > *yw* (**A**), *GMR* > *SerT*-IR (**A'**), and *GMR* > *SerT*-IR/*diap1* (**A"**). Quantification of EdU-positive cells in the posterior region surrounded by dotted lines (**B**). DAPI staining of the nuclei of cone cells of third-instar larvae carrying *GMR* > *yw* (**C**) and *GMR* > *SerT*-IR (**C'**). Arrows point to the abnormal formation of the nuclei. Posterior region of third-instar larvae carrying *GMR* > *yw* and *GMR* > *SerT*-IR, respectively, were stained with anti-phosphorylated-histone 3 (Ser10) antibody conjugated with Alexa488 (**D**,**D'**) and with anti-phosphorylated-gamma-Histone 2A antibody (**F**,**F'**). Quantification of pH3S10-positive cells and γ-H2AV-positive cells in the region surrounded by dotted lines, respectively (**E**,**G**). Scale bars indicate 100 μm (**A**–**A"**,**D**,**D'**,**F**,**F'**) and 5 μm (**C**,**C'**). The triangles indicate the MF. a, anterior; p, posterior. ****, $p < 0.0001$; ***, $p < 0.001$; n.s., not significant.

2.4. SerT Knockdown Induces a Rough Eye Phenotype via the PI3K/Akt Pathway

We suspected that the eye phenotype of the *SerT* knockdown fly might be

influenced by the PI3k/Akt pathway. This pathway is well known to be involved in the regulation of the cell cycle, and there is also evidence that suggests its participation in the neurogenesis of the compound eye [22]. First, we visualized the Akt activation level using specific *Drosophila* anti-phosphorylated Akt at Ser505 (the equivalent of human Ser473). Figure 4A–D" shows a significant decrease in the level of phosphorylated Akt in the posterior region (the region affected by *SerT*-kd, Figure 4D–D") of the eye disc of the *SerT*-kd fly compared with that in the control (Figure 4A–B") and in the anterior region (the region unaffected by *SerT*-kd, Figure 4C–C") of the same eye disc.

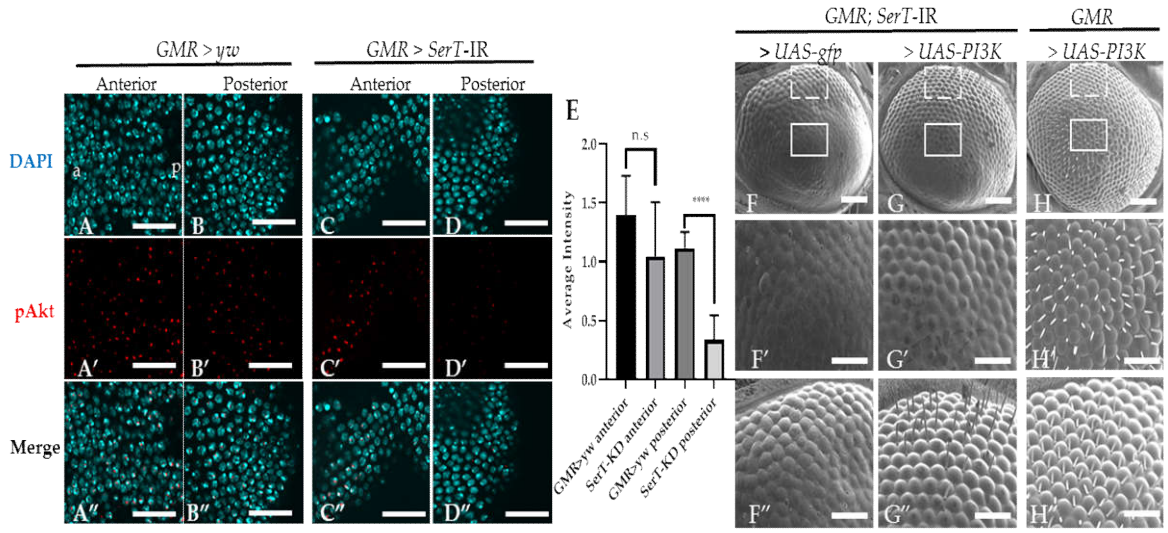

Figure 4. Knockdown of *SerT* reduces the levels of phosphorylated Akt protein. The anterior and posterior region to the MF in the eye discs of third-instar larvae carrying GMR > yw as a control (**A**–**A"**,**B**–**B"**, respectively) and GMR > *SerT*-IR as *SerT*-kd (**C**–**C"**,**D**–**D"**, respectively) were stained with DAPI (blue) and anti-phosphorylated-Akt antibody followed by secondary antibodies labeled with Alexa594 (red). Merged images are also shown (**A"**,**B"**,**C"**,**D"**). The images are representative of 5 eye imaginal discs. Quantification of the phosphorylated Akt average intensity (**E**). Scanning electron micrograph of the adult compound eyes of flies carrying *GMR*-Gal4/Y, *SerT*-IR/UAS-*gfp*, + (**F**), *GMR*-Gal4/Y, *SerT*-IR/UAS-*PI3K*, + (**G**), and *GMR*-Gal4/Y, UAS-*PI3K*, + (**H**). Larger images of regions surrounded by box and dotted lines are shown (**F'**–**H'**,**F"**–**H"**, respectively).

Scale bar indicates 15μm (**A–D”**), 100 μm (**F–H**) and 30 μm (**F’–H”**). a, anterior; p, posterior; ****, $p < 0.0001$.

Since Akt activation is regulated via PI3K, we tried to rescue the phenotype by introducing *PI3K* in *SerT*-kd flies. The result showed the significant restoration of ommatidia shape and bristle formation (Figure 4G–G”), compared with those in the control flies carrying *gfp* (Figure 4F–F”). A representative image of the compound eyes of flies with *PI3K* overexpression, but without *SerT*-RNAi, is also shown (Figure 4H–H”). Taken together, the results indicated that the levels of Akt phosphorylation were reduced by *SerT* knockdown. The levels of phosphorylated Akt are negatively regulated by the feedback of Akt itself, and it is often difficult to interpret changes in Akt phosphorylation. This observation alone is not proof of reduced PI3K/Akt activity, but it is suggestive.

3. Discussion

SerT plays important roles in various processes in the peripheral system [30]. In this study, we visualized the expression of SerT in *Drosophila* imaginal disc by specific antibody (Figure 1B,B’), which led us to elucidate the function of SerT in eye development. The effect of the knockdown of the *SerT* gene using a *GMR*-GAL4 driver resulted in a noticeable rough eye phenotype, represented by the abnormal organization of ommatidia and the complete loss of bristles (Figure 1D,D’,E,E’). Previous studies indicated that the rough eye phenotype was possibly caused by the disruption of the cell cycle in the development of the compound eyes, which may lead to the premature termination of cells via a caspase-dependent pathway [27,31]. Our results indeed showed an increase in caspase-dependent cell death in knockdown flies, which was effectively rescued by the caspase inhibitor DIAP1 or p35 (Figure 2D–D”,E–E”). Figure 3A’ also showed that, under *SerT*-kd, the number of cells in the S-phase accumulated in the posterior region was significantly higher in knockdown flies than in the control, though the first mitotic wave (indicated by MF) and the second wave had passed.

Although a large number of cells were in S-phase, pH3S10 staining showed no

change in the number of cells undergoing mitosis between *SerT*-kd and the controls. A previous study showed that *rux* mutation caused defects in the cell cycle regulation that led to the premature entry into S phase (represented by substantial increases in 5-bromo-2'-deoxyuridine staining), resulting in a similar but more severe rough eye phenotype to that observed in the present study and in the absence of changes in mitosis [32]. Moreover, our recent study of the regulation of the developing wing suggested that the knockdown of dLipin by an *sd*-GAL4 driver induces the accumulation of cells in S-phase while also decreasing the number of mitotic cells [33]. These studies suggest that increases in S- and M-phase cells can be regulated differently due to cell cycle defects; however, the underlying mechanism needs to be investigated further. The result shown in Figure 3F,F', describing a lack of DNA damage, excludes the involvement of the DNA-repair mechanism in the phenotype. An alternative hypothesis might be that the excess numbers of S-phase cells might be induced by compensatory mechanisms related to cell death. Although this is suggestive, key evidence is missing, especially the cause of differential regulation of the mitotic phase. The abnormal organization of cone cell nuclei (Figure 3C') suggested that excessive S-phase proliferation may cause the elevated recruitment of DNA in this cell type, strengthening our claim in the link between S-phase proliferation and rough eye phenotype. However, whether extra cone cells are formed or not is unclear and requires further investigation.

Then, our results suggested that the excessive caspase-dependent cell death in the posterior region of the eye disc was induced by the decreased level of the PI3K/Akt pathway activation. Clinical and experimental data highlighted the insulin-induced PI3K/Akt pathway, a universal pathway in yeast, insects, mice, and mammals, as a common pathway in the stabilization of cell growth under the control of nutrition [34]. The PI3K/Akt pathway is widely known as a crucial inhibitor of apoptotic effectors in the growth-signaling pathway. The activation of this pathway can reduce apoptosis in various types of cells, including neuronal, ischemia-inducing myocardial, and tumor cells [35–38]. In the rat hippocampus,

the PI3K/Akt signaling pathway plays a pivotal role in neuronal apoptosis after inducing subarachnoid hemorrhage [39]. Furthermore, the inhibition of the PI3K/Akt pathway promotes the activation of caspase-3, subsequently increasing apoptotic cell death in diabetic rats [40]. Moreover, the activation of PI3K/Akt is effectively controlled by the insulin network [41,42]. The inhibition of SerT via a genetic or pharmacological mechanism results in insulin resistance prior to adiposity [43–45]. Previous research revealed that in SerT-deficient mice, JNK activity is exalted, and insulin-induced Akt activation is declined, whereas the elevation of AKT signaling by PTEN deficiency rescues the glucose tolerance phenotype. This study also claimed that SerT-deficiency downregulates insulin action and is responsible for impaired PI3K/Akt signaling in the peripheral system [43]. Consistent with these previous findings, our study also showed a link between SerT and PI3K/Akt signaling.

SerT functions are tightly connected to serotonin. SerT knockdown will diminish the clearance of excessive serotonin, which may, in turn, elevates the serotonin accumulation in cells. In mammals, serotonin induces the synthesis and release of insulin, as well as enhances the sensitivity of its target tissue [46]. In *Drosophila*, serotonergic neurons express a GTPase NS3, which controls growth via insulin signaling. Furthermore, Nässel et al. provided a more detailed mechanism that one of the serotonin receptors, 5-HT1A, inhibits adenylate cyclase and protein kinase A, thus inactivating cAMP response element-binding protein, which in turn stimulates insulin signaling [47]. Multiple studies showed that increasing serotonin levels activates the PI3K/Akt pathway in cancer cells and neurodegenerative Parkinson's disease cellular model [48,49]. This discrepancy can be explained by the different serotonin regulatory processes in serotonergic network interactions. The serotonergic system is complex and regulated by multiple factors, and the regulatory feedback caused by excessive serotonin levels have been previously recorded [50,51]. In order to clarify the detailed interaction within the serotonergic system, the assay of serotonin levels in *SerT* knockdown flies is further needed. Further studies to reveal the specific cell types affected by

SerT during eye disc development are warranted.

In conclusion, the cell fate of *Drosophila* imaginal eye disc is strictly regulated by a series of events, and numerous molecules have been found to control these events. In this study, we showed that the cell death induced by the suppressed activation of the PI3K/Akt pathway resulted in a rough eye phenotype in *SerT*-kd flies. Thus, we concluded that SerT played a role in normal eye development by controlling caspase-dependent cell death through the PI3K/Akt pathway. The detailed mechanism of the link between SerT and this cascade requires further investigations.

4. Materials and Methods

4.1. Fly Stocks

Fly stocks were maintained at 25 °C on standard food containing 0.65% agar, 10% glucose, 4% dry yeast, and 5% cornmeal. Transgenic flies with UAS-*dSerT*-IR$_{686–1079}$ (*SerT*-IR1) and UAS-*dSerT*-IR$_{1740–1760}$ (*SerT*-IR2) were obtained from the Vienna *Drosophila* Resource Center (#100584; Vienna, Austria) and Bloomington *Drosophila* Stock Center (#62985; Bloomington, IN, USA), respectively. These flies carried an IR of the *SerT* gene (targeting regions from nucleotide 686 to 1079 and from 1740 to 1760, respectively) downstream of the UAS sequence, on the second chromosome. All other flies used in this study were obtained from Bloomington *Drosophila* Stock Center: UAS-*gfp* (#1522), UAS-*p35* (#5072), UAS-*diap1* (#6657), UAS-*PI3K* (#8287). *yw* flies were used as the wild-type strain.

4.2. Scanning Electron Microscopy

All flies were anesthetized by CO_2 and mounted on a holder. A VE-7800 scanning electron microscope (Keyence, Osaka, Japan) was used to observe the compound eyes of adult flies. At least five adult male flies were observed in each experiment.

4.3. Immunostaining

Cells in the S-phase were detected using Click-iT EdU (5-ethynyl-2′-deoxyuridine) labeling Alexa Fluor 594 Imaging Kit (Invitrogen, Carlsbad, CA,

USA) [33]. Third instar larvae were dissected in phosphate buffer saline (PBS), and the eye discs were fixed in 4% paraformaldehyde for 20 min at 25 °C. After washing with PBS containing 0.3% Triton X-100 (PBST), the samples were blocked with 0.1% PBST and 10% normal goat serum for 30 min at 25 °C, and incubated with diluted primary antibodies in 0.1% PBST and 10% normal goat serum for 16 h at 4 °C [52,53]. The following antibodies were used as primary antibodies: rabbit anti-*Drosophila* SerT antibody (1:200; S1001-25H, USBio, Salem, MA, USA), rabbit anti-cleaved caspase-3 antibody (1:500; Sigma-Aldrich, St. Louis, MO, USA), anti-Phospho-Histone H3 (Ser10) (D2C8) XP Rabbit mAb conjugated with Alexa488 (1:400; Cell Signaling Technology, Danvers, MA, USA), anti-phosphorylated-histone 2A gamma variant antibody (1:400; DSHB, Iowa, IA, USA), and anti-phosphorylated-*Drosophila* Akt (Ser505) antibody (1:200; Cell Signaling Technology, Danvers, MA, USA). After washing with 0.3% PBST, samples were incubated with secondary antibodies labeled with either Alexa488 or Alexa 594 (Goat anti-rabbit IgG 1:1000 and Goat anti-mouse IgG 1:800; Abcam, Cambridge, UK) for 2 h at 25 °C. After further washing with 0.1% PBST, samples were mounted in a Vectashield mounting medium (Vector Laboratories, Burlingame, CA, USA) and observed by using a Fluoview Fv10i-0 confocal laser scanning microscope (Olympus, Tokyo, Japan). The signals were analyzed by the MetaMorph software (Molecular Devices, Sunnyvale, CA, USA).

4.4. Statistical Analysis

Signals in the posterior region of the MF were counted from at least six eye imaginal discs. All experiments were repeated at least three times. Statistical analyses were performed using the Student's *t*-test and one-way ANOVA. Error bars represent the standard error of the mean (SEM), and all the data are shown as means ± SEM. Differences with *p*-values of <0.05 were considered significant.

5. References

1. Rillich, J.; Stevenson, P.A. Serotonin Mediates Depression of Aggression After Acute and Chronic Social Defeat Stress in a Model Insect. *Front. Behav. Neurosci.* **2018**, *12*, doi:10.3389/fnbeh.2018.00233.
2. Lin, S.H.; Lee, L.T.; Yang, Y.K. Serotonin and mental disorders: A concise review on molecular neuroimaging evidence. *Clin. Psychopharmacol. Neurosci.* **2014**, *12*, 196–202, doi:10.9758/cpn.2014.12.3.196.
3. Carhart-Harris, R.L.; Nutt, D.J. Serotonin and brain function: A tale of two receptors. *J. Psychopharmacol.* **2017**, *31*, 1091–1120.
4. Jacobs, B.L.; Azmitia, E.C. Structure and function of the brain serotonin system. *Physiol. Rev.* **1992**, *72*, 165–229.
5. Visser, A.K.; Ramakrishnan, N.K.; Willemsen, A.T.; Di Gialleonardo, V.; de Vries, E.F.; Kema, I.P.; Dierckx, R.A.; van Waarde, A. [(11)C]5-HTP and microPET are not suitable for pharmacodynamic studies in the rodent brain. *J. Cereb. Blood Flow Metab.* **2014**, *34*, 118–125, doi:10.1038/jcbfm.2013.171.
6. Terry, N.; Margolis, K.G. Serotonergic mechanisms regulating the GI tract: Experimental evidence and therapeutic relevance. *Handb. Exp. Pharmacol.* **2017**, *239*, 319–342, doi:10.1007/164_2016_103.
7. Oh, C.M.; Namkung, J.; Go, Y.; Shong, K.E.; Kim, K.; Kim, H.; Park, B.Y.; Lee, H.W.; Jeon, Y.H.; Song, J.; et al. Regulation of systemic energy homeostasis by serotonin in adipose tissues. *Nat. Commun.* **2015**, *6*, 6794, doi:10.1038/ncomms7794.
8. Brindley, R.L.; Bauer, M.B.; Blakely, R.D.; Currie, K.P. Serotonin and Serotonin Transporters in the Adrenal Medulla: A Potential Hub for Modulation of the Sympathetic Stress Response. *ACS Chem. Neurosci.* **2017**, doi:10.1021/acschemneuro.7b00026.
9. Genet, N.; Billaud, M.; Rossignol, R.; Dubois, M.; Gillibert-Duplantier, J.;

Isakson, B.E.; Marthan, R.; Savineau, J.P.; Guibert, C. Signaling Pathways Linked to Serotonin-Induced Superoxide Anion Production: A Physiological Role for Mitochondria in Pulmonary Arteries. *Front. Physiol.* **2017**, *8*, 76, doi:10.3389/fphys.2017.00076.

10. Solmi, M.; Gallicchio, D.; Collantoni, E.; Correll, C.U.; Clementi, M.; Pinato, C.; Forzan, M.; Cassina, M.; Fontana, F.; Giannunzio, V.; et al. Serotonin transporter gene polymorphism in eating disorders: Data from a new biobank and META-analysis of previous studies. *World J. Biol. Psychiatry* **2016**, *17*, 244–257, doi:10.3109/15622975.2015.1126675.
11. Yamakawa, K.; Matsunaga, M.; Isowa, T.; Ohira, H. Serotonin transporter gene polymorphism modulates inflammatory cytokine responses during acute stress. *Sci. Rep.* **2015**, *5*, 13852, doi:10.1038/srep13852.
12. Haase, J.; Grudzinska-Goebel, J.; Muller, H.K.; Munster-Wandowski, A.; Chow, E.; Wynne, K.; Farsi, Z.; Zander, J.F.; Ahnert-Hilger, G. Serotonin Transporter Associated Protein Complexes Are Enriched in Synaptic Vesicle Proteins and Proteins Involved in Energy Metabolism and Ion Homeostasis. *ACS Chem. Neurosci.* **2017**, doi:10.1021/acschemneuro.6b00437.
13. Thanh, M.T.; Pham, T.L.A.; Tran, B.D.; Nguyen, Y.D.H.; Kaeko, K. Drosophila model for studying the link between lipid metabolism and development. *Front. Biosci. (Landmark Ed.)* **2020**, *25*, 147–158.
14. Treisman, J.E. Retinal differentiation in Drosophila. *Wiley Interdiscip. Rev. Dev. Biol.* **2013**, *2*, 545–557, doi:10.1002/wdev.100.
15. Escudero, L.M.; Freeman, M. Mechanism of G1 arrest in the Drosophila eye imaginal disc. *BMC Dev. Biol.* **2007**, *7*, 13, doi:10.1186/1471-213X-7-13.
16. Sukhanova, M.J.; Du, W. Control of cell cycle entry and exiting from the second mitotic wave in the Drosophila developing eye. *BMC Dev. Biol.* **2008**, *8*, 7, doi:10.1186/1471-213X-8-7.
17. Meserve, J.H.; Duronio, R.J. A population of G2-arrested cells are selected as sensory organ precursors for the interommatidial bristles of the

Drosophila eye. *Dev. Biol.* **2017**, *430*, 374–384, doi:10.1016/j.ydbio.2017.06.023.

18. Baker, N.E.; Li, K.; Quiquand, M.; Ruggiero, R.; Wang, L.H. Eye development. *Methods* **2014**, *68*, 252–259, doi:10.1016/j.ymeth.2014.04.007.
19. Zhang, H.; Stallock, J.P.; Ng, J.C.; Reinhard, C.; Neufeld, T.P. Regulation of cellular growth by the Drosophila target of rapamycin dTOR. *Genes Dev.* **2000**, *14*, 2712–2724, doi:10.1101/gad.835000.
20. Wang, B.; Chen, N.; Wei, Y.; Li, J.; Sun, L.; Wu, J.; Huang, Q.; Liu, C.; Fan, C.; Song, H. Akt signaling-associated metabolic effects of dietary gold nanoparticles in Drosophila. *Sci. Rep.* **2012**, *2*, 1–7, doi:10.1038/srep00563.
21. Palomero, T.; Sulis, M.L.; Cortina, M.; Real, P.J.; Barnes, K.; Ciofani, M.; Caparros, E.; Buteau, J.; Brown, K.; Perkins, S.L.; et al. Mutational loss of PTEN induces resistance to NOTCH1 inhibition in T-cell leukemia. *Nat. Med.* **2007**, *13*, 1203–1210, doi:10.1038/nm1636.
22. Bateman, J.M. Mechanistic insights into the role of mTOR signaling in neuronal differentiation. *Neurogenesis* **2015**, *2*, e1058684.
23. Hietakangas, V.; Cohen, S.M. Re-evaluating AKT regulation: Role of TOR complex 2 in tissue growth. *Genes Dev.* **2007**, *21*, 632–637, doi:10.1101/gad.416307.
24. Slade, J.D.; Staveley, B.E. Compensatory growth in novel Drosophila Akt1 mutants Developmental Biology. *BMC Res. Notes* **2015**, *8*, 77, doi:10.1186/s13104-015-1032-0.
25. Giang, T.; Rauchfuss, S.; Ogueta, M.; Scholz, H. The Serotonin Transporter Expression in *Drosophila melanogaster*. *J. Neurogenet.* **2011**, *25*, 17–26, doi:10.3109/01677063.2011.553002.
26. Hidalgo, S.; Molina-Mateo, D.; Escobedo, P.; Zárate, R.V.; Fritz, E.; Fierro, A.; Perez, E.G.; Iturriaga-Vasquez, P.; Reyes-Parada, M.; Varas, R.; et al. Characterization of a Novel *Drosophila* SERT Mutant: Insights on the Contribution of the Serotonin Neural System to Behaviors. *ACS Chem.*

Neurosci. **2017**, *8*, 2168–2179, doi:10.1021/acschemneuro.7b00089.

27. Tanaka, R.; Miyata, S.; Yamaguchi, M.; Yoshida, H. Role of the smallish gene during Drosophila eye development. *Gene* **2019**, *684*, 10–19, doi:10.1016/j.gene.2018.10.056.
28. Ly, L.L.; Suyari, O.; Yoshioka, Y.; Tue, N.T.; Yoshida, H.; Yamaguchi, M. DNF-YB plays dual roles in cell death and cell differentiation during Drosophila eye development. *Gene* **2013**, *520*, 106–118, doi:10.1016/j.gene.2013.02.036.
29. Lake, C.M.; Holsclaw, J.K.; Bellendir, S.P.; Sekelsky, J.; Hawley, R.S. The development of a monoclonal antibody recognizing the Drosophila melanogaster phosphorylated histone H2A variant (γ-H2AV). *G3 (Bethesda)* **2013**, *3*, 1539–1543, doi:10.1534/g3.113.006833.
30. Watanabe, H.; Rose, M.; Kanayama, Y.; Shirakawa, H.; Aso, H. Energy Homeostasis by the Peripheral Serotonergic System. In *Serotonin—A Chemical Messenger Between All Types of Living Cells*; InTech: 2017.
31. Rimkus, S.A.; Katzenberger, R.J.; Trinh, A.T.; Dodson, G.E.; Tibbetts, R.S.; Wassarman, D.A. Mutations in String/CDC25 inhibit cell cycle re-entry and neurodegeneration in a Drosophila model of Ataxia telangiectasia. *Genes Dev.* **2008**, *22*, 1205–1220, doi:10.1101/gad.1639608.
32. Thomas, B.J.; Gunning, D.A.; Cho, J.; Zipursky, S.L. Cell cycle progression in the developing Drosophila eye: Roughex encodes a novel protein required for the establishment of G1. *Cell* **1994**, *77*, 1003–1014, doi:10.1016/0092-8674(94)90440-5.
33. Duy Binh, T.; L. A. Pham, T.; Nishihara, T.; Thanh Men, T.; Kamei, K. The Function of Lipin in the Wing Development of Drosophila melanogaster. *Int. J. Mol. Sci.* **2019**, *20*, 3288, doi:10.3390/ijms20133288.
34. Juarez-Carreño, S.; Morante, J.; Dominguez, M. Systemic signalling and local effectors in developmental stability, body symmetry, and size. *Cell Stress* **2018**, *2*, 340–361, doi:10.15698/cst2018.12.167.
35. Zheng, L.; Ren, J.Q.; Li, H.; Kong, Z.L.; Zhu, H.G. Downregulation of

wild-type p53 protein by HER-2/neu mediated PI3K pathway activation in human breast cancer cells: Its effect on cell proliferation and implication for therapy. *Cell Res.* **2004**, *14*, 497–506, doi:10.1038/sj.cr.7290253.

36. Noshita, N.; Lewén, A.; Sugawara, T.; Chan, P.H. Evidence of phosphorylation of Akt and neuronal survival after transient focal cerebral ischemia in mice. *J. Cereb. Blood Flow Metab.* **2001**, *21*, 1442–1450, doi:10.1097/00004647-200112000-00009.
37. Noshita, N.; Lewén, A.; Sugawara, T.; Chan, P.H. Akt phosphorylation and neuronal survival after traumatic brain injury in mice. *Neurobiol. Dis.* **2002**, *9*, 294–304, doi:10.1006/nbdi.2002.0482.
38. Xu, X.; Cao, Z.; Cao, B.; Li, J.; Guo, L.; Que, L.; Ha, T.; Chen, Q.; Li, C.; Li, Y. Carbamylated erythropoietin protects the myocardium from acute ischemia/reperfusion injury through a PI3K/Akt-dependent mechanism. *Surgery* **2009**, *146*, 506–514, doi:10.1016/j.surg.2009.03.022.
39. Zhuang, Z.; Zhao, X.; Wu, Y.; Huang, R.; Zhu, L.; Zhang, Y.; Shi, J. The anti-apoptotic effect of PI3K-Akt signaling pathway after subarachnoid hemorrhage in rats. *Ann. Clin. Lab. Sci.* **2011**, *41*, 364–372.
40. Meng, Y.; Wang, W.; Kang, J.; Wang, X.; Sun, L. Role of the PI3K/AKT signalling pathway in apoptotic cell death in the cerebral cortex of streptozotocin-induced diabetic rats. *Exp. Ther. Med.* **2017**, *13*, 2417–2422, doi:10.3892/etm.2017.4259.
41. Kulkarni, M.M.; Kulkarni, M.M.; Sopko, R.; Sun, X.; Hu, Y.; Nand, A.; Villalta, C.; Moghimi, A.; Yang, X.; Mohr, S.E.; et al. An Integrative Analysis of the InR/PI3K/Akt Network Identifies the Dynamic Response to Insulin Signaling. *Cell Rep.* **2016**, *16*, 3062–3074, doi:10.1016/j.celrep.2016.08.029.
42. Galagovsky, D.; Katz, M.J.; Acevedo, J.M.; Sorianello, E.; Glavic, A.; Wappner, P. The Drosophila insulin-degrading enzyme restricts growth by modulating the PI3K pathway in a cell-autonomous manner. *Mol. Biol. Cell* **2014**, *25*, 916–924, doi:10.1091/mbc.E13-04-0213.

43. Chen, X.; Margolis, K.J.; Gershon, M.D.; Schwartz, G.J.; Sze, J.Y. Reduced serotonin reuptake transporter (SERT) function causes insulin resistance and hepatic steatosis independent of food intake. *PLoS ONE* **2012**, *7*, doi:10.1371/journal.pone.0032511.

44. Zha, W.; Ho, H.T.B.; Hu, T.; Hebert, M.F.; Wang, J. Serotonin transporter deficiency drives estrogen-dependent obesity and glucose intolerance. *Sci. Rep.* **2017**, *7*, 1–14, doi:10.1038/s41598-017-01291-5.

45. Giannaccini, G.; Betti, L.; Palego, L.; Marsili, A.; Santini, F.; Pelosini, C.; Fabbrini, L.; Schmid, L.; Giusti, L.; Maffei, M.; et al. The expression of platelet serotonin transporter (SERT) in human obesity. *BMC Neurosci.* **2013**, *14*, 128, doi:10.1186/1471-2202-14-128.

46. Lam, D.D.; Heisler, L.K. Serotonin and energy balance: Molecular mechanisms and implications for type 2 diabetes. *Expert Rev. Mol. Med.* **2007**, *9*, 1–24.

47. Nässel, D.R.; Kubrak, O.I.; Liu, Y.; Luo, J.; Lushchak, O.V. Factors that regulate insulin producing cells and their output in drosophila. *Front. Physiol.* **2013**, *4*, 252, doi:10.3389/fphys.2013.00252.

48. Dizeyi, N.; Hedlund, P.; Bjartell, A.; Tinzl, M.; Austild-Taskén, K.; Abrahamsson, P.A. Serotonin activates MAP kinase and PI3K/Akt signaling pathways in prostate cancer cell lines. *Urol. Oncol. Semin. Orig. Investig.* **2011**, *29*, 436–445, doi:10.1016/j.urolonc.2009.09.013.

49. Nakano, N.; Matsuda, S.; Ichimura, M.; Minami, A.; Ogino, M.; Murai, T.; Kitagishi, Y. PI3K/AKT signaling mediated by G protein-coupled receptors is involved in neurodegenerative Parkinson's disease (Review). *Int. J. Mol. Med.* **2017**, *39*, 253–260.

50. Bari, A.; Theobald, D.E.; Caprioli, D.; Mar, A.C.; Aidoo-Micah, A.; Dalley, J.W.; Robbins, T.W. Serotonin modulates sensitivity to reward and negative feedback in a probabilistic reversal learning task in rats. *Neuropsychopharmacology* **2010**, *35*, 1290–1301, doi:10.1038/npp.2009.233.

51. Daubert, E.A.; Heffron, D.S.; Mandell, J.W.; Condron, B.G. Serotonergic dystrophy induced by excess serotonin. *Mol. Cell. Neurosci.* **2010**, *44*, 297–306, doi:10.1016/j.mcn.2010.04.001.
52. Binh, T.D.; Pham, T.L.A.; Men, T.T.; Dang, T.T.P.; Kamei, K. LSD-2 dysfunction induces dFoxO-dependent cell death in the wing of Drosophila melanogaster. *Biochem. Biophys. Res. Commun.* **2019**, *509*, 491–497, doi:10.1016/j.bbrc.2018.12.132.
53. Binh, T.D.; Pham, T.L.A.; Men, T.T.; Kamei, K. Dysfunction of LSD-1 induces JNK signaling pathway-dependent abnormal development of thorax and apoptosis cell death in Drosophila melanogaster. *Biochem. Biophys. Res. Commun.* **2019**, *516*, 451–456, doi:10.1016/j.bbrc.2019.06.075.

CONCLUSIONS

In this thesis, I investigate the function of two genes, *Lipin* and *SerT*, in development by tissue-specific knockdown in the developing wing and eye, respectively, of these genes in *Drosophila melanogaster* model.

Chapter 1:

In this chapter, I can successfully visualized Lipin expression in the eye disc of *Drosophila* 3rd-instar larvae. Specifically, we showed that the tissue-selective knockdown of *dLipin* in the wing pouch led to an atrophied wing. Elevated DNA damage was observed in the wing imaginal disc of *dLipin*-knockdown flies. dLipin dysfunction induced accumulation of cells in S phase and significantly reduced the number of mitotic cells, indicating DNA damage-induced activation of the G2/M checkpoint. Reduced expression of cyclin B, which is critical for the G2 to M transition, was observed in the margin of the wing imaginal disc of *dLipin*-knockdown flies. The knockdown of *dLipin* led to increased apoptotic cell death in the wing imaginal disc. Thus, our results suggest that dLipin is involved in DNA replication during normal cell cycle progression in wing development of *Drosophila melanogaster*.

Chapter 2:

SerT in the brain is an important neurotransmitter transporter involved in mental health. However, its role in peripheral organs is poorly understood. In this study, we investigated the function of SerT in the development of the compound eye in *Drosophila melanogaster*. We found that SerT knockdown led to excessive cell death and an increased number of cells in S-phase in the posterior eye imaginal disc. Furthermore, the knockdown of *SerT* in the eye disc suppressed the activation of Akt, and the introduction of *PI3K* effectively rescued this phenotype. These results suggested that SerT plays a role in the healthy eye development of *D. melanogaster* by controlling cell death through the regulation of the PI3K/Akt pathway. This research further confirm the the involvement of

SerT in peripheral system. It also open a suggestion to the possible explanation of side effects of SerT-targeted anti-depressant drugs in human.

LIST OF PUBLICATIONS

1. **The Function of Lipin in the Wing Development of *Drosophila melanogaster***

Tran Duy Binh, Tuan L.A. Pham, Taisei Nishihara, Tran Thanh Men and Kaeko Kamei

International Journal of Molecular Sciences, 20, 3288, 2019; https://doi.org/10.3390/ijms20133288

2. **Role of Serotonin Transporter in Eye Development of *Drosophila melanogaster***

Tuan L.A. Pham, Tran Duy Binh, Guanchen Liu, Thanh Q.C. Nguyen, Yen D.H. Nguyen, Ritsuko Sahashi, Tran Thanh Men and Kaeko Kamei

International Journal of Molecular Sciences, 21, 4086, 2020; https://doi.org/10.3390/ijms21114086

ACKNOWLEDGEMENTS

I would like to express my deepest thanks to my supervisor, Prof. Dr. Kaeko Kamei, who gave me an opportunity study in Japan, for her supervision, guidance and support through my research and my life in Kyoto. Without her support and guidance, it would be impossible for me to complete the project.

I would like to express my sincere thanks to all Professors, staff at Kyoto Institute of Technology for their support during my study and working on the research project.

I am deeply indebted to the Ministry of Education, Culture, Sports, Science and Technology (MEXT) and Kyoto Institute of Technology for providing the financial support and scholarship which made it possible for me to study at Kyoto Institute of Technology

Last but not least, words cannot express my deepest gratitude to my beloved family: my parents, my wife, my brother and my little boy; Vietnamese friends and lab-mates, the main source of my strength and moving-force to overcome obstacles facing in my life.